Appendix for Online Publication

A Proofs of analytical results

We first provide proofs of the analytical results in the main text.

A.1 Proposition 1

Proof. Combining (14) and (18), wealth evolves according to

$$\begin{aligned} W_t = (1-\exp(-\xi))\bar{W} + \\ \exp(-\xi)\exp(r_{t-1})\left[W_{t-1} + (\alpha \log P_{t-1} + \theta_{t-1})\left(\exp(-r_t - r_{t-1} - \log P_{t-1}) - 1\right)\right]. \end{aligned}$$

Around the stochastic steady-state, this implies

$$\begin{aligned} d\log W_t = \frac{\exp(-\xi)\exp(\bar{r})\left[W - X\right]}{W} dr_{t-1} + \exp(-\xi)\exp(\bar{r}) d\log W_{t-1} + \\ \frac{\exp(-\xi)\exp(\bar{r})\left(\exp(-2\bar{r} - \log P) - 1\right)}{W} d\theta_{t-1} - \frac{\exp(-\xi) X \exp(-\bar{r} - \log P)}{W} dr_t + \\ \frac{\exp(-\xi)\exp(\bar{r})\left[\alpha\left(\exp(-2\bar{r} - \log P) - 1\right) - X\exp(-2\bar{r} - \log P)\right]}{W} d\log P_{t-1}. \quad (27) \end{aligned}$$

The impact response of wealth to a short rate shock follows, with

$$D \equiv \frac{X}{W}\exp(-\bar{r} - \log P)$$

summarizing the duration of arbitrageurs' wealth. □

A.2 Proposition 2

Proof. (14) and (11) imply

$$\begin{aligned} E_t r^{(2)}_{t+1} &= -E_t r_{t+1} - \log P_t, \\ &= -\kappa_r \bar{r} - (1-\kappa_r) r_t - \log P_t \end{aligned}$$

Substituting these into (17) yields

$$-\kappa_r \bar{r} - (2-\kappa_r) r_t - \log P_t + \frac{1}{2}\sigma_r^2 = \frac{\alpha \log P_t + \theta_t}{W_t}\sigma_r^2.$$

This implies that around the stochastic steady-state

$$d\log P_t = -\frac{2-\kappa_r}{1+\frac{1}{W}\alpha\sigma_r^2} dr_t - \frac{\frac{1}{W}\sigma_r^2}{1+\frac{1}{W}\alpha\sigma_r^2} d\theta_t + \frac{\frac{X}{W}\sigma_r^2}{1+\frac{1}{W}\alpha\sigma_r^2} d\log W_t. \tag{28}$$

It follows from (19) that

$$df_t = \frac{1-\kappa_r-\frac{1}{W}\alpha\sigma_r^2}{1+\frac{1}{W}\alpha\sigma_r^2} dr_t + \frac{\frac{1}{W}\sigma_r^2}{1+\frac{1}{W}\alpha\sigma_r^2} d\theta_t - \frac{\frac{X}{W}\sigma_r^2}{1+\frac{1}{W}\alpha\sigma_r^2} d\log W_t. \tag{29}$$

The response of the forward rate to a short rate shock follows from Proposition 1. □

B Empirical appendix

We now provide supplementary empirical results accompanying those in section 4.

B.1 Effects of monetary shocks on real forwards

We focus in the paper on the effects of monetary shocks on real forwards paying through 10 years in the future. Here we describe the set of outstanding TIPS which motivate this choice, and we provide scatterplots which correspond to our baseline regression results.

Figure 8 displays outstanding TIPS issues at each month through 2019 by their remaining time to maturity (updating Figure 1 in Gurkaynak et al. (2008) through more recent data). The figure demonstrates that after 2004, there have been multiple outstanding TIPS securities with remaining maturity below five years; at all dates, there have been multiple outstanding securities with remaining maturity between five and 10 years. Since there are fewer issues at maturities above 10 years, we focus on maturities two through 10 years to avoid the concern that our findings are driven by changes in liquidity premia rather than term premia.

Figure 9 visually depicts the relationship between the change in the 10-year real forward rate and the monetary-induced change in the one-year ahead one-year forward

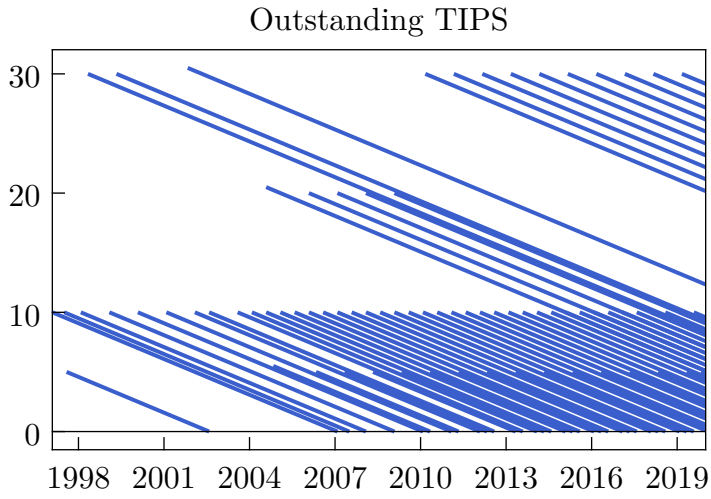

Figure 8: remaining time to maturity of TIPS outstanding

Notes: at each point in time, we plot the set of TIPS outstanding by time to maturity. We obtain this data using the auction query on Treasury Direct to search for all TIPS by original issue date and original time to maturity. There were no buybacks of TIPS during this period.

rate reported in the baseline specification in Table 1. It makes evident that the positive relationship is not driven by any one observation.

B.2 Effects of monetary shocks on forecast revisions

As discussed in the main text, one interpretation of the response of long-dated real forwards to a monetary tightening is that it reflects a "Fed information" effect. If a surprise monetary tightening reveals news about a stronger than expected economy and thus higher expected real interest rate five to 10 years ahead, it can explain our estimated forward responses without requiring a change in term premia.

Here we cast doubt on this interpretation using the response of professional forecasts in the Blue Chip Economic Indicators around FOMC announcements, consistent with the arguments in Bauer and Swanson (2023b). Forecasters from major financial institutions and businesses are surveyed at the beginning of each month regarding major economic indicators over the remaining quarters of the year and quarters over the subsequent year. For a given month, we compute the change in the average forecast (the "forecast revision") of a particular indicator at a particular quarter in the future from the beginning of that month to the beginning of the subsequent month. We then project this forecast revision onto the sum of monetary surprises over that month.

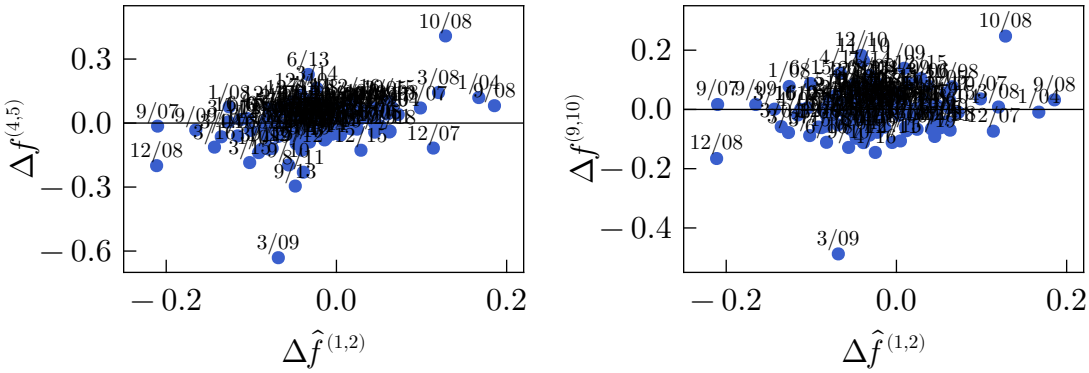

Figure 9: $\Delta f_t^{(4,5)}$ and $\Delta f_t^{(9,10)}$ on $\widehat{\Delta f_t^{(1,2)}}$

Notes: $\widehat{\Delta f_t^{(1,2)}}$ is estimated based on first-stage projection on high-frequency monetary surprise from Bauer and Swanson (2023a).

Table 6 reports the effect of monetary surprises on forecast revisions for the unemployment rate, annualized quarter-over-quarter real GDP growth, and annualized quarter-over-quarter CPI growth, all of which are expressed in percentage points. We follow Bauer and Swanson (2023b) in considering an average of the forecast revisions for one quarter ahead, two quarters ahead, and three quarters ahead.

The message from this table echoes that in Bauer and Swanson (2023b). In our baseline specification, a surprise monetary tightening is associated with expectations of higher unemployment, lower GDP growth, and lower CPI inflation. The fact that we orthogonalize the monetary surprise measure with respect to macroeconomic and financial news available prior to the FOMC announcement is important in revealing these effects: without orthogonalizing the monetary surprise in the fourth row, each of these point estimates would flip signs. Consistent with the interpretation in Bauer and Swanson (2023b), this suggests that part of the monetary surprise is the market learning about the Fed's reaction function to this news, and part of it is a true surprise innovation to the Taylor rule. By orthogonalizing the surprise with respect to macro news known prior to the announcement, we are focusing on only the effects of the surprise innovation to the Taylor rule, not the effects of the macro news itself, on forecast revisions. Looking across all other specifications (again using orthogonalized measures of monetary surprises), we find broadly similar results to our baseline specification: a monetary tightening is associated with a weaker economy and lower inflation.[63]

[63]Unlike in Bauer and Swanson (2023b), these responses tend not to be significantly different from

Specification	Unemp rate	Real GDP growth	CPI inflation
Baseline	0.24	-0.57	-0.31
	(0.27)	(0.36)	(0.18)
Excl. 7/08-6/09	-0.14	0.06	-0.11
	(0.18)	(0.25)	(0.14)
Excl. days w. LSAP news	0.48	-0.66	-0.49
	(0.32)	(0.48)	(0.19)
Without orthogonalizing IV	-0.35	0.20	0.04
	(0.30)	(0.31)	(0.14)
Swanson (2021b) Fed funds IV	0.30	-0.72	-0.18
	(0.55)	(0.52)	(0.31)
Jarocinski and Karadi (2020a) IV	0.36	-0.75	-0.25
	(0.36)	(0.38)	(0.24)
Nakamura and Steinsson (2018a) IV	0.00	-0.40	-0.36
	(0.42)	(0.63)	(0.39)
Swanson (2021b) forward guidance IV	0.21	-0.45	-0.24
	(0.19)	(0.31)	(0.14)

Table 6: Blue Chip forecast revisions on $\Delta f_t^{(1,2)}$, instrumented by high-frequency surprise

Notes: forecast revisions for one- through three-quarters ahead are averaged, as in Bauer and Swanson (2023b). Since forecasts are made monthly, the forecast revision is regressed on the cumulative one-day change in one-year ahead one-year real forward around FOMC announcements, instrumented by cumulative high-frequency monetary surprise, within each month. Robust standard errors provided in parenthesis.

These responses of forecast revisions are inconsistent with the interpretation that a monetary tightening conveys news about higher expected growth and thus a higher real interest rate in the medium/long run. Conversely, they are fully consistent with a monetary tightening conveying news about lower expected inflation, helping to explain the response of forward breakeven inflation rates described in the next subsection.

B.3 Effects of monetary shocks on nominal yield curve

In the main text we study the implications of monetary shocks on real forwards. Here we replicate our analysis using the nominal yield curve. We use Gurkaynak et al. (2006)'s interpolated nominal yield curve, maintained and updated by the Federal

zero, however. We expect that this is because Bauer and Swanson (2023b) effectively orthogonalize with respect to an even broader set of macro news variables than we do.

Specification	$\Delta f_t^{(3,4)}$	$\Delta f_t^{(5,6)}$	$\Delta f_t^{(7,8)}$	$\Delta f_t^{(9,10)}$
Baseline	0.57	0.28	0.11	0.02
	(0.10)	(0.13)	(0.13)	(0.11)
Excl. 7/08-6/09	0.53	0.06	-0.15	-0.24
	(0.12)	(0.14)	(0.15)	(0.16)
Excl. days w. LSAP news	0.48	0.17	0.02	-0.05
	(0.13)	(0.16)	(0.15)	(0.13)
Without orthogonalizing IV	0.62	0.34	0.17	0.06
	(0.10)	(0.15)	(0.16)	(0.14)
Swanson (2021b) Fed funds IV	0.53	-0.08	-0.30	-0.29
	(0.33)	(0.32)	(0.34)	(0.30)
Jarocinski and Karadi (2020a) IV	0.46	0.14	-0.01	-0.07
	(0.13)	(0.14)	(0.14)	(0.12)
Nakamura and Steinsson (2018a) IV	0.67	0.29	0.08	-0.00
	(0.12)	(0.21)	(0.25)	(0.25)
Swanson (2021b) forward guidance IV	0.72	0.54	0.36	0.21
	(0.09)	(0.10)	(0.09)	(0.08)

Table 7: $\Delta f_t^{(\tau-1,\tau),nom}$ on $\Delta f_t^{(1,2)}$, instrumented by high-frequency surprise

Notes: $f_t^{(\tau-1,\tau),nom}$ denotes nominal forward rate. Robust standard errors provided in parenthesis.

Reserve, to compute yields and forwards at a daily frequency. We focus on the same January 2004 through December 2019 period used in our analysis of the real yield curve only to maintain comparability with those results. Data for the nominal yield curve is available earlier and we obtain similar results over the broader sample.

Table 7 summarizes the response of nominal one-year forwards to a $1pp$ increase in the one-year ahead one-year real forward, instrumented by the monetary surprise. We maintain the same first stage outcome variable to maintain comparability with the results for real forwards in Table 1. Table 8 summarizes the responses of the nominal less real forwards, which equal forward breakeven inflation rates. As is made especially clear by the latter table, the response of nominal forwards is dampened at all maturities, reflected in a decline of forward breakeven inflation rates.

These results are in turn consistent with the decline in survey-based measures of expected inflation around FOMC announcements described in the prior subsection. To further dive into the expected inflation response, Table 9 reports the Blue Chip forecast revisions for CPI inflation by quarter. Across specifications in virtually all quarters (except without orthogonalizing the monetary surprise), a surprise tightening lowers expected inflation. These effects remain economically substantial for the forecasts

Specification	$\Delta f_t^{(3,4)}$	$\Delta f_t^{(5,6)}$	$\Delta f_t^{(7,8)}$	$\Delta f_t^{(9,10)}$
Baseline	-0.16	-0.20	-0.19	-0.17
	(0.06)	(0.08)	(0.08)	(0.07)
Excl. 7/08-6/09	-0.15	-0.29	-0.26	-0.19
	(0.09)	(0.11)	(0.10)	(0.10)
Excl. days w. LSAP news	-0.19	-0.27	-0.25	-0.19
	(0.08)	(0.10)	(0.09)	(0.08)
Without orthogonalizing IV	-0.14	-0.19	-0.18	-0.18
	(0.06)	(0.11)	(0.10)	(0.08)
Swanson (2021b) Fed funds IV	-0.03	-0.36	-0.41	-0.32
	(0.25)	(0.30)	(0.32)	(0.23)
Jarocinski and Karadi (2020a) IV	-0.12	-0.18	-0.18	-0.15
	(0.09)	(0.11)	(0.11)	(0.08)
Nakamura and Steinsson (2018a) IV	-0.17	-0.12	-0.05	-0.07
	(0.15)	(0.17)	(0.15)	(0.15)
Swanson (2021b) forward guidance IV	-0.12	-0.07	-0.06	-0.07
	(0.05)	(0.06)	(0.06)	(0.06)

Table 8: $\Delta(f_t^{(\tau-1,\tau),nom} - f_t^{(\tau-1,\tau)})$ on $\Delta f_t^{(1,2)}$, instrumented by high-frequency surprise

Notes: $f_t^{(\tau-1,\tau),nom}$ denotes nominal forward rate. Robust standard errors provided in parenthesis.

six quarters ahead. We note that the magnitudes are comparable to the response of breakeven forward inflation rates as reported in Table 8.

A decline in expected inflation upon a monetary tightening is consistent with the predictions of standard New Keynesian models at short horizons, and a decline in the expected inflation target at long horizons. The latter is consistent with the arguments in Gurkaynak et al. (2005b) and Gurkaynak, Sack, and Swanson (2005a) that monetary surprises contain news about the central bank's long-run inflation target. Changes in the long-run inflation target will have no direct effects on long maturity real forwards, underscoring the importance of focusing on the real yield curve to uncover the effects of monetary shocks on term premia.

With that said, the effects of monetary policy shocks on the nominal yield curve are still important for the results in our paper because most of the fixed income assets traded in practice are nominal. In this context, it is important to note that nominal *yields* rise on impact of a monetary tightening far out into the yield curve, as shown for our baseline specification in Figure 10, even though long-dated nominal forward rates fall. Similar results are obtained for the alternative specifications described above. We conclude that a monetary tightening will lower the wealth of agents having positive

	Quarters ahead					
Specification	1	2	3	4	5	6
Baseline	-0.64	-0.14	-0.15	-0.10	-0.06	-0.20
	(0.43)	(0.11)	(0.10)	(0.07)	(0.13)	(0.14)
Excl. 7/08-6/09	-0.16	-0.09	-0.08	0.01	-0.08	-0.24
	(0.29)	(0.15)	(0.14)	(0.09)	(0.14)	(0.14)
Excl. days w. LSAP news	-1.01	-0.25	-0.20	-0.10	-0.02	-0.15
	(0.49)	(0.14)	(0.11)	(0.09)	(0.18)	(0.16)
Without orthogonalizing IV	0.18	-0.02	-0.04	-0.01	0.09	-0.06
	(0.32)	(0.14)	(0.10)	(0.12)	(0.18)	(0.16)
Swanson (2021b) Fed funds IV	-0.58	-0.13	0.17	-0.17	-0.32	-0.56
	(0.71)	(0.20)	(0.12)	(0.14)	(0.21)	(0.14)
Jarocinski and Karadi (2020a) IV	-0.58	-0.15	-0.01	-0.13	-0.19	-0.47
	(0.54)	(0.13)	(0.13)	(0.08)	(0.14)	(0.10)
Nakamura and Steinsson (2018a) IV	-0.43	-0.27	-0.39	-0.40	-0.30	-0.64
	(0.86)	(0.30)	(0.30)	(0.17)	(0.25)	(0.31)
Swanson (2021b) forward guidance IV	-0.40	-0.12	-0.21	-0.08	-0.05	0.06
	(0.35)	(0.10)	(0.09)	(0.09)	(0.12)	(0.11)

Table 9: Blue Chip CPI inflation forecast revisions on $\Delta f_t^{(1,2)}$, instrumented by high-frequency surprise

Notes: since forecasts are made monthly, the forecast revision is regressed on the cumulative one-day change in one-year ahead one-year real forward around FOMC announcements, instrumented by cumulative high-frequency monetary surprise, within each month. Robust standard errors provided in parenthesis.

duration in nominal bonds, so long as the duration is not extremely high.

B.4 Estimating equity duration

In the main text we compute arbitrageur duration using the balance sheets of broker/dealers and hedge funds together with estimates of duration by asset class. For corporate equities, we estimate duration using the approach proposed in Greenwald et al. (2023), which uses the Gordon growth formula together with the valuation ratio on the stock market. We motivate this approach here.

Suppose an equity claim trading at price P pays an instantaneous dividend D that grows at constant growth rate g. Let r denote the instantaneous and constant short

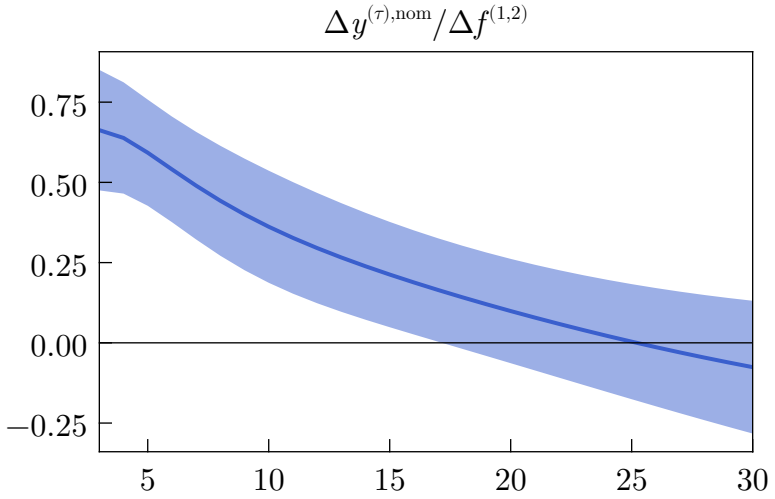

Figure 10: $\Delta y_t^{(\tau),nom}$ on $\Delta f_t^{(1,2)}$, instrumented by high-frequency surprise

Notes: $y_t^{(\tau),nom}$ denotes nominal yield. At each integer τ on the x-axis, we plot coefficient and 95% confidence interval using $\Delta y_t^{(\tau),nom}$ as the outcome variable. Confidence intervals based on robust standard errors.

rate. The price of the asset is then

$$P = \int_0^\infty D \exp((g-r)t)dt = \frac{D}{r-g}.$$

Then the modified duration of the equity claim, the percentage change in the equity price given a 1% permanent change in r, is given by

$$-\frac{\partial P}{\partial r}\frac{1}{P} = \frac{1}{r-g} = \frac{P}{D}.$$

One issue in implementing this formula is that the corporate payout ratio has fallen over time, as firms shift to buying back shares rather than paying dividends. This would raise the price/dividend ratio and thus our estimate of duration, even though the underlying duration of cashflows earned by the equity owner may be unchanged.[64] For this reason, in our baseline estimation of duration we instead assume that the equity owner receives income (inclusive of buybacks) which is a constant fraction κ of earnings, which in turn grows at constant rate g. Similar logic as above implies that

[64]That said, van Binsbergen (2024) provides arguments that support using the price/dividend ratio to estimate duration even in the presence of buybacks. We consider the present approach to be conservative, as we demonstrate in the next subsection.

modified duration is then

$$-\frac{\partial P}{\partial r}\frac{1}{P} = \frac{1}{\kappa}\frac{P}{E}.$$

We use the time series of the price/earnings ratio for the S&P 500, obtained from Robert Shiller's website, together with a payout ratio of $\kappa = 0.5$, to obtain our baseline estimate of duration each quarter. The payout ratio of 0.5 is the average ratio of dividends to earnings over 1950-1990 before share buybacks grew in importance. In the next subsection we consider the sensitivity of our duration estimate to the assumed payout ratio, or to using the price/dividend ratio instead.

B.5 Sensitivity of estimated arbitrageur duration

In this appendix we assess the sensitivity of our balance sheet-based estimates of arbitrageur duration along several dimensions.

Representative portfolio within asset class One simplifying assumption we make is that within asset classes, arbitrageurs hold a representative portfolio with duration given by market-wide benchmarks.

We can evaluate this assumption for Treasuries in particular. For these securities, the Primary Dealer Statistics provide information on net positions by reasonably granular maturity buckets. We compute the average duration of Treasuries held by dealers as a weighted average of duration by maturity bucket, with weights given by dealers' position in each bucket. For instance, given the maturity buckets reported prior to 2013, we compute

$$PDDUR_t \equiv \frac{0.5Q_{(TB)t} + 1.5Q_{(m\leq 3)t} + 4.5Q_{(3<m\leq 6)t} + 8.5Q_{(6<m\leq 11)t} + 14Q_{(11<m)t}}{Q_{(TB)t} + Q_{(m\leq 3)t} + Q_{(3<m\leq 6)t} + Q_{(6<m\leq 11)t} + Q_{(11\leq m)t}},$$

where $Q_{(TB)t}$ is the dollar value of Treasury bills held, $Q_{(m\leq 3)t}$ is the dollar value of Treasury bonds held with remaining maturity less than or equal to three years, and so on. When dealers' total position in Treasuries is close to zero, $PDDUR_t$ can become very imprecise, so we code it as missing when it falls outside $[-30, 30]$.

Figure 11 plots $PDDUR_t$ (weekly, given the reporting frequency of the Primary Dealer Statistics) against the daily Bloomberg index of average duration of marketable Treasuries outstanding. We see that $PDDUR_t$ tracks the Bloomberg index quite well until the financial crisis, and between 2015-2019. It is much more volatile during the crisis, consistent with dealers' small net position in Treasuries during this time as it

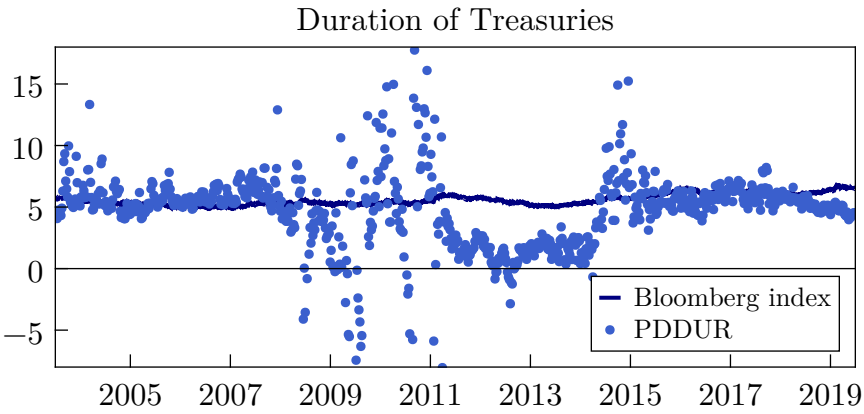

Figure 11: duration of Treasuries

Notes: $PDDUR_t$ coded as missing when it falls outside $[-30, 30]$, which only occurs when dealers' total position in Treasuries is close to zero.

flipped sign (Du, Hebert, and Li (2023), Hanson, Malkhozov, and Venter (2024)). In 2012-2015, it is below the Bloomberg index.

We conclude that using the Bloomberg index does not do a bad job summarizing dealers' average Treasury duration over our sample period. The second and seventh rows of Table 10 report how our estimated average duration of arbitrageurs over 2012-2019 changes when we replace the Bloomberg Treasury index with $PDDUR_t$, both when we include equities and exclude equities from the calculation.[65] Consistent with the above discussion, our estimates of duration fall, but only slightly.

At the same time, we note from Figure 11 that $PDDUR_t$ is much more volatile than the Bloomberg index (even outside the financial crisis, in which volatility may reflect measurement error given dealers' small net position). This means that while our use of the Bloomberg index may not do a bad job in estimating dealers' average duration over this period, it almost surely understates the volatility in their duration.

Derivatives exposure A lack of comprehensive data on derivatives is a major downside of constructing arbitrageurs' duration using balance sheet data, as acknowledged in the main text.

For Treasury futures, however, we can make more progress in assessing the magnitude of this problem using the positions in Treasury futures reported in the CFTC Traders in Financial Futures report. Figure 12 compares the cash position in Treasuries

[65] As in our benchmark calculations using the Bloomberg index, we assign $PDDUR_t$ to the duration of hedge funds' position in Treasuries as well, in the absence of a concrete alternative.

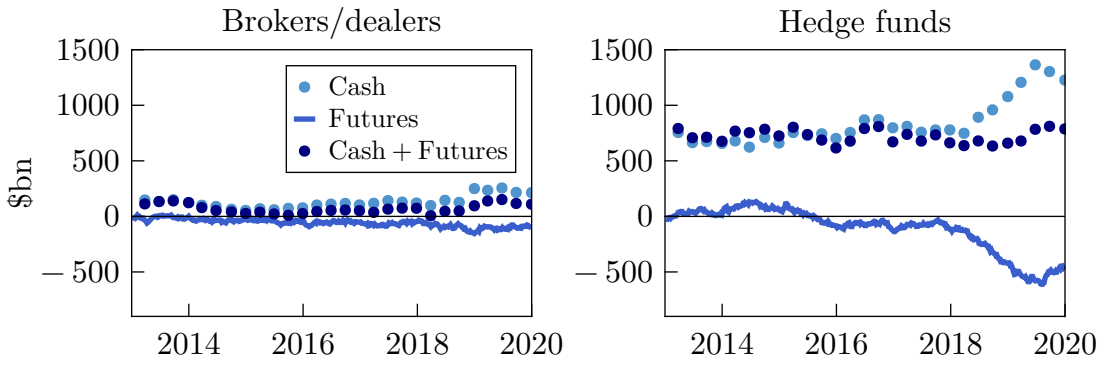

Figure 12: cash and futures positions in Treasuries

Notes: cash position is from Financial Accounts for dealers and Form PF (provided in Enhanced Financial Accounts) for hedge funds, as reported in Table 2. Futures positions are from CFTC Traders in Financial Futures report for dealers and leveraged funds (which we map to hedge funds).

from the Financial Accounts (for dealers) and Form PF (for hedge funds) with the net futures positions in Treasuries from this CFTC report for these same sectors (hedge funds corresponding to "leveraged funds" in the CFTC report).[66] We also sum up the cash position and net futures position, reflecting the net position in Treasuries.

There are several takeaways from this figure. Both dealers and leveraged funds have been net short Treasury futures since 2015. As a fraction of their cash position, the net futures position of dealers is greater in magnitude, suggesting that dealers hold little economic exposure to Treasury yields. But the magnitude of hedge funds' exposure is much larger than dealers (consistent with the relative size of their balance sheets evident from Table 2), and hedge funds are net long Treasuries throughout this period. Indeed, the main consequence of accounting for Treasury futures is that the run-up in hedge funds' cash positions starting in 2018 is offset by a run-up in their futures positions, consistent with rising positions in the Treasury cash/futures basis trade. We conclude that the basis trade is sizeable in the last couple years of our sample, but it does not play a very important role for most of our sample period.

It is also natural to add in the Treasury futures data to our measured balance sheets and adjust our estimates of average duration appropriately.[67] The third and

[66]The raw Form PF data in fact combines cash and futures positions because this is how the survey is worded. The Enhanced Financial Accounts from which we are able to access this data reports the cash positions alone.

[67]We assume the duration of an individual security is the midpoint of the deliverable maturity buckets, following Jansen et al. (2024). This implies duration of 1.875 for the 2Y Treasury Note future; 4.7 for the 5Y Treasury Note future; 7.125 for the 10Y Treasury Note future; 9.7 for the Ultra

Incl equities	Use PD Treasury duration	Incl Treasury futures	Equity duration	Avg duration, Q4 2012–Q4 2019
yes	no	no	$(1/0.5)P/E$	28.0
yes	yes	no	$(1/0.5)P/E$	27.8
yes	yes	yes	$(1/0.5)P/E$	28.7
yes	no	no	$(1/0.6)P/E$	24.1
yes	no	no	P/D	32.3
no	no	no	n/a	10.3
no	yes	no	n/a	9.9
no	yes	yes	n/a	10.1

Table 10: duration of arbitrageurs

Notes: duration in first and sixth rows estimated as described in Table 2. Remaining rows consider alternative measures of duration for specific asset classes or include derivatives data on Treasury futures.

eighth rows of Table 10 indicate that, perhaps surprisingly, netting out dealers' and leverage funds' positions in Treasury futures in fact slightly raises average duration over 2012-2019. Intuitively, there are two effects of netting out futures positions. The first is that it lowers arbitrageurs' duration of assets in the numerator, and the second is that it lowers arbitrageurs' value of net wealth in the denominator (because they are net short Treasury futures). When the duration of Treasury futures is less than what we estimate for arbitrageurs' wealth excluding futures, the latter effect dominates the former and duration accounting for futures in fact rises. In any case, this effect is not especially large because the magnitude of Treasury futures is still smaller than the cash Treasury positions, which are in turn only a subset of arbitrageurs' overall positions.

Equity duration The fourth and fifth rows of Table 10 finally illustrate the sensitivity of our duration estimates to alternative estimates for equity duration. We first consider a higher payout ratio of 0.6, which lowers our estimate for equity duration following the argument in the prior section.[68] Even in this case, we estimate average duration of 24.1. We next consider using the price/dividend ratio rather than price/earnings ratio. In this case, we estimate average duration of 32.3. While there is

10Y Treasury Note future; 20 for the Treasury Bond future; and 30 for the Ultra Treasury Bond future.

[68]This is a high payout ratio: there were only 33 months between 1950-1990 (before share buybacks grew in importance) with a payout ratio at least this high.

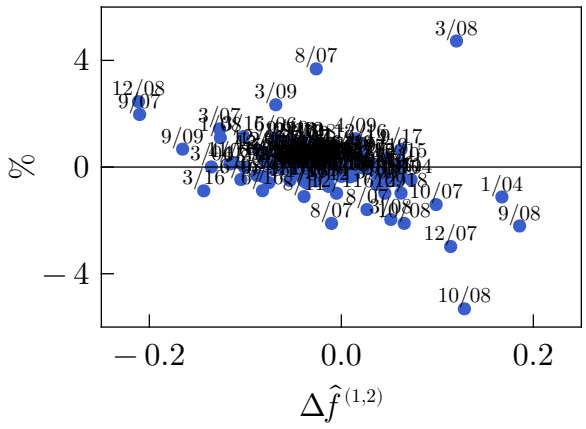

Figure 13: change in dealer equity prices on $\widehat{\Delta f_t^{(1,2)}}$

Notes: $\widehat{\Delta f_t^{(1,2)}}$ is estimated based on first-stage projection on high-frequency monetary surprise estimated by Bauer and Swanson (2023a).

substantial uncertainty about the true duration of equities, we conclude that the order of magnitude of arbitrageur duration including equities is indeed likely around 30.

B.6 Effects of monetary shocks on dealer equities

The main text presented the high-frequency response of dealer equities to a monetary surprise in our baseline and alternative specifications. Here we provide more details on this analysis.

Table 11 provides the list of primary dealers whose stock price responses around FOMC announcements are studied. This list is constructed by obtaining the list of past and continuing dealers from the Federal Reserve Bank of New York, and then identifying the subset of these for which we can find the relevant CRSP/TAQ data.

Figure 13 visually depicts the relationship between the change in dealer equity prices and the change in the one-year ahead one-year forward induced by the monetary surprise in the baseline specification. As with the response of the long-dated real forwards, no single observation drives the estimated relationship.

B.7 Broader evidence of wealth revaluation channel

We finally present broader evidence of the wealth revaluation channel, which was summarized in section 4.3 in the main text.

Dealer	Ticker	Availability
Bank of America	BAC	1/2/2004-12/31/2019
Barclays	BCS	1/2/2004-12/31/2019
BMO	BMO	1/2/2004-12/31/2019
Bank of Novia Scotia	BNS	1/2/2004-12/31/2019
Bear Stearns	BSC	1/2/2004-5/30/2008
Citigroup	C	1/2/2004-12/31/2019
CIBC	CM	1/2/2004-12/31/2019
Credit Suisse	CS	1/2/2004-12/31/2019
Deutsche Bank	DB	1/2/2004-12/31/2019
Goldman Sachs	GS	1/2/2004-12/31/2019
HSBC	HSBC	1/2/2004-12/31/2019
Jefferies	JEF	1/2/2004-2/28/2013
JP Morgan	JPM	1/2/2004-12/31/2019
Lehman Brothers	LEH	1/2/2004-9/17/2008
Merrill Lynch	MER	1/2/2004-12/31/2008
MF Global	MF	7/19/2007-10/28/2011
Mizuho	MFG	11/8/2006-12/31/2019
Morgan Stanley	MS	1/2/2004-12/31/2019
Nomura	NMR	1/2/2004-12/31/2019
Banc One	ONE	1/2/2004-6/30/2004
Prudential	PRU	1/2/2004-12/31/2019
RBS	RBS	10/18/2007-12/31/2019
RBC	RY	1/2/2004-12/31/2019
TD	TD	1/2/2004-12/31/2019
UBS	UBS	1/2/2004-12/31/2019
Wells Fargo	WFC	1/2/2004-12/31/2019
Zions First National	ZION	1/2/2004-12/31/2019

Table 11: dealers with stock market data

Monetary surprises and intermediation capacity We first provide additional evidence that a monetary tightening reduces intermediation capacity in fixed income markets. Table 12 summarizes the evidence.

The first column demonstrates that a monetary tightening lowers the capital risk factor of He et al. (2017). This is the daily innovation to primary dealers' capital ratio when modeled as an AR(1) process relative to the lagged capital ratio, which He et al. (2017) demonstrate is a priced risk factor. In our baseline specification, a monetary tightening which raises the one-year ahead one-year forward by $1pp$ is associated with a $9.7pp$ decline in this risk factor. This is a similar magnitude as our estimated high frequency decline in dealer stock prices, which is sensible since these are closely related.

Specification	PD capital risk factor	Δ Excess bond premium	Δ Yield curve noise	Δ 5-yr USD/G10 CIP dev.
Baseline	-9.7	1.1	1.4	-3.9
	(4.9)	(0.6)	(1.0)	(2.0)
Excl. 7/08-6/09	-9.6	0.6	0.0	-1.5
	(7.9)	(0.4)	(0.5)	(1.3)
Excl. days w. LSAP news	-13.7	1.4	1.1	-4.1
	(5.8)	(0.7)	(1.3)	(2.7)
Without orthogonalizing IV	-13.2	0.1	1.5	-2.6
	(5.2)	(0.4)	(1.0)	(1.3)
Swanson (2021b) Fed funds IV	-0.7	1.1	7.0	-4.3
	(16.6)	(0.6)	(3.4)	(4.2)
Jarocinski and Karadi (2020a) IV	-5.7	1.2	2.4	-4.2
	(7.6)	(0.6)	(1.3)	(2.3)
Nakamura and Steinsson (2018a) IV	-12.0	1.3	1.8	-1.6
	(12.0)	(1.3)	(1.5)	(2.2)
Swanson (2021b) forward guidance IV	-5.4	0.8	0.1	-3.2
	(3.7)	(0.5)	(0.5)	(1.8)

Table 12: change in financial conditions on $\Delta f_t^{(1,2)}$, instrumented by high-frequency surprise

Notes: primary dealers capital risk factor is from He et al. (2017), excess bond premium is from Gilchrist and Zakrajsek (2012), yield curve noise is from Hu et al. (2013), and CIP deviations are from Du et al. (2018a), all of which are updated through 2019. All measures except excess bond premium are changes from day before announcement to day after announcement. Excess bond premium is measured only monthly so second column regresses monthly change in excess bond premium on cumulative one-day change in one-year ahead one-year real forward around FOMC announcements, instrumented by cumulative high-frequency monetary surprise, within each month. Robust standard errors provided in parenthesis.

The second column demonstrates that a monetary tightening raises the excess bond premium as constructed by Gilchrist and Zakrajsek (2012). This is the credit spread on corporate bonds not attributable to default risk, and is a widely used measure of risk appetite in the corporate bond market. In our baseline specification, a monetary tightening which raises the one-year ahead one-year forward by $1pp$ is associated with $1.1pp$ increase in the excess bond premium. This is consistent with the findings of other papers employing VARs or local projections (e.g., Gertler and Karadi (2015) and Bauer and Swanson (2023a)), which also find that this increase in the excess bond premium persists for several quarters after the monetary surprise.

The third column demonstrates that a monetary tightening raises the yield curve noise measure of Hu et al. (2013). This is the root mean squared error in Treasury bond yields around a smoothed yield curve, reflecting diminished intermediation capacity and thus liquidity in the Treasury market. In our baseline specification, a monetary tightening which raises the one-year ahead one-year forward by $1pp$ is associated with a $1.4bp$ increase in yield curve noise. While this is not statistically significantly different from zero at conventional levels (unlike the other responses in Table 12), it becomes significant when using other measures of monetary surprises.

The fourth column demonstrates that a monetary tightening also widens the average five-year deviation from covered interest parity (CIP) between U.S. and G10 currency countries from Du et al. (2018a).[69] This is the five year dollar LIBOR rate less the synthetic dollar LIBOR rate, given by the foreign currency LIBOR rate plus the forward currency premium. In our baseline specification, a monetary tightening which raises the one-year ahead one-year forward by $1pp$ is associated with a $3.9bp$ widening of the average CIP deviation.

Exploiting the panel of CIP deviations The panel structure of CIP deviations provides particularly convincing evidence that a monetary surprise tightens the balance sheet constraint faced by arbitrageurs, as because their wealth has fallen. Table 13 projects the change in the five-year CIP deviation between the U.S. and each G10 currency country on the change in the one-year ahead one-year real forward, an indicator for a positive CIP deviation preceding the monetary announcement, and their interaction, instrumented by the high-frequency monetary surprise and its interaction with the same indicator variable. Across all specifications, a monetary tightening causes the CIP deviation to fall for currencies with an initially negative CIP deviation, and rise for currencies with an initially positive CIP deviation. All coefficients in the table are significantly different from zero at conventional levels.

This pattern of a widening CIP deviation away from zero is particularly consistent with a tightening of arbitrageurs' balance sheet constraints upon a positive monetary surprise. To see this, it is useful to consider an extension of the simplified environment studied in section 3 which effectively integrates the model of CIP deviations in Du

[69]The G10 currency countries are Australia, Canada, Denmark, the Euro Area (aggregated across members), Japan, New Zealand, Norway, Sweden, Switzerland, and the U.K. The average USD/G10 CIP deviation was essentially zero prior to the global financial crisis, and negative since then (except for two days in 2018). Thus, a decline in the average CIP deviation means a widening of the basis.

	$\widehat{\Delta f_t^{(1,2)}}$	$\widehat{\Delta f_t^{(1,2)}} \times$ (pos dev.)$_{t-1}$
Baseline	-5.7	7.5
	(1.5)	(2.3)
Excl. 7/08-6/09	-2.1	3.9
	(0.9)	(1.4)
Excl. days w. LSAP news	-5.1	5.3
	(2.1)	(2.6)
Without orthogonalizing IV	-4.6	8.3
	(1.0)	(2.7)
Swanson (2021b) Fed funds IV	-6.9	11.1
	(2.7)	(4.4)
Jarocinski and Karadi (2020a) IV	-6.0	7.9
	(1.7)	(2.6)
Nakamura and Steinsson (2018a) IV	-4.7	10.0
	(2.1)	(3.4)
Swanson (2021b) forward guidance IV	-4.6	5.2
	(1.4)	(1.8)

Table 13: change in 5-yr CIP deviation on $\Delta f_t^{(1,2)}$, indicator for positive deviation, and interaction, instrumented by high-frequency surprise

Notes: change in CIP deviation measured from day before announcement to day after announcement, as in Table 12. Each row reports coefficients on change in one-year ahead one-year real forward and its interaction with indicator for positive deviation. Robust standard errors provided in parenthesis.

et al. (2018b) with our preferred habitat model of the yield curve.

Suppose the arbitrageurs described in section 3 can trade an additional asset, a "synthetic dollar bond" paying rate r_t^*, which reflects the one-period yield on a bond in foreign currency swapped into dollars (neither the foreign short rate or forward currency premium being explicitly modeled).[70] The only difference between this bond and the dollar one-period bond is that the former is subject to a balance sheet constraint, as motivated by the evidence in Du et al. (2018b). Letting x_t^* denote the individual arbitrageur's position in this synthetic bond, the balance sheet constraint is

$$|x_t^*| \leq \kappa^* w_t, \tag{30}$$

for $\kappa^* > 0$, which captures the idea that a decline in arbitrageur wealth will tighten

[70]More formally, swapped into dollars should be understood here to mean swapped into the U.S. consumption bundle, since we interpret our model in fully real terms.

the constraint. The arbitrageur's evolution of wealth is now

$$w_{t+1} = w_t \exp(r_t) + x_t \left(\frac{\exp(-r_{t+1})}{P_t} - \exp(r_t) \right) + x_t^* \left(\exp(r_t^*) - \exp(r_t) \right).$$

Finally, we assume that habitat investors demand the synthetic dollar bond according to

$$Z_t^* = \alpha^* r_t^* - \theta_t^*,$$

where $\alpha^* > 0$. The second term is the latent demand for borrowing in the synthetic dollar bond that arbitrageurs must accommodate, say because there is latent demand by households and firms abroad to borrow in synthetic dollars to hedge dollar assets. The first term reflects that these other agents will be price elastic and borrow less in synthetic dollars if the cost of doing so rises. Market clearing requires

$$X_t^* + Z_t^* = 0,$$

where X_t^* denotes the aggregate position of arbitrageurs in the synthetic dollar bond. The rest of the environment is unchanged from that in section 3.

We now obtain the following results for the CIP deviation $r_t - r_t^*$, the proof of which we present at the end of this subsection:

Proposition 3. *Suppose κ^* is sufficiently small that (30) is binding. Then if arbitrageurs are long synthetic dollar bonds ($X_t^* > 0$, which will be the case for θ_t^* sufficiently positive):*

- *the CIP deviation is negative ($r_t - r_t^* < 0$);*
- *and a decline in arbitrageur wealth lowers the CIP deviation ($\frac{d[r_t - r_t^*]}{dW_t} > 0$).*

If arbitrageurs are short synthetic dollar bonds ($X_t^* < 0$, which will be the case for θ_t^* sufficiently negative):

- *the CIP deviation is positive ($r_t - r_t^* > 0$);*
- *and a decline in arbitrageur wealth raises the CIP deviation ($\frac{d[r_t - r_t^*]}{dW_t} < 0$).*

Hence, a widening of the CIP deviation regardless of its initial sign is consistent with a tightening of arbitrageurs' balance sheet constraint due to lower wealth. To the

extent that arbitrageurs are long two-period bonds, their wealth will indeed fall if the short rate rises, as demonstrated in the main text.

Note that another reason CIP deviations may change in response to a short rate shock is if habitat demand for synthetic bonds changes. The analog of "reaching for yield" in this context would be if habitat investors' demand was instead

$$Z_t^* = \alpha^*(r_t^* - r_t) - \theta_t^*.$$

In this case, it is straightforward to show that a rise in the short rate would mechanically lower the CIP deviation regardless of its initial sign, since habitat investors would seek to borrow more in synthetic dollar bonds. In this way, evidence of a widening of the CIP deviation away from zero for both initially positive and negative bases is uniquely consistent with a change in the tightness of arbitrageurs' balance sheet constraint.

State-dependent effects of monetary shocks We finally provide additional evidence of a distinctive prediction of our theory: when arbitrageurs' wealth is low and thus duration is high (all else equal), the conditional effect of a monetary tightening on long-dated real forwards is amplified.

Table 14 projects the change in the 10-year forward on the change in the one-year ahead one-year real forward, a proxy for arbitrageurs' intermediation capacity preceding the monetary announcement, and their interaction, instrumented by the high-frequency monetary surprise and its interaction with the same state variable. Each state variable is scaled by its standard deviation in sample, and defined so that an increase corresponds to a decline in intermediation capacity.

The first four columns of Table 14 correspond to the asset price-based measures of intermediation capacity studied earlier in this appendix. In our baseline specification, a one standard deviation higher value of primary dealers' leverage (the inverse of the He et al. (2017) intermediary capital ratio) is associated with a $0.14pp$ larger response of the 10-year forward to a monetary tightening which raises the one-year ahead one-year forward by $1pp$. A one standard deviation higher value of the excess bond premium, yield curve noise measure, and five-year CIP deviation (in absolute value) are associated with a $0.16pp$, $0.13pp$, and $0.16pp$ larger response of this same forward rate, respectively. The stronger response of the 10-year forward in all of these cases is both statistically and economically significant, recalling that the average response of the 10-year forward in Table 1 was $0.19pp$. Similarly strong results are obtained

	State variable				
	PD leverage	Excess bond premium	Yield curve noise	− 5-yr CIP dev.	FA, Form PF dur.
Baseline	0.14	0.16	0.13	0.16	0.32
	(0.05)	(0.04)	(0.03)	(0.07)	(0.23)
Excl. 7/08-6/09	-0.25	-0.09	-0.21	0.06	0.32
	(0.13)	(0.11)	(0.20)	(0.09)	(0.23)
Excl. days w. LSAP news	-0.01	0.11	0.08	0.09	0.32
	(0.09)	(0.09)	(0.06)	(0.08)	(1.02)
Without orthogonalizing IV	0.14	0.11	0.08	0.16	-0.06
	(0.05)	(0.03)	(0.03)	(0.08)	(0.15)
Swanson (2021b) Fed funds IV	0.40	2.05	0.30	0.27	-0.60
	(0.29)	(14.09)	(0.36)	(0.10)	(0.58)
Jarocinski and Karadi (2020a) IV	0.29	0.23	0.14	0.19	1.15
	(0.12)	(0.07)	(0.04)	(0.09)	(1.23)
Nakamura and Steinsson (2018a) IV	0.15	0.16	0.14	0.24	-0.22
	(0.09)	(0.05)	(0.05)	(0.12)	(0.79)
Swanson (2021b) forward guidance IV	0.13	0.14	0.12	0.12	0.06
	(0.05)	(0.03)	(0.03)	(0.08)	(0.12)

Table 14: $\Delta f_t^{(9,10)}$ on $\Delta f_t^{(1,2)}$, state variable, and interaction, instrumented by high-frequency surprise

Notes: all state variables measured prior to monetary announcement and scaled by standard deviation over sample period. Each cell reports the estimated coefficient on the interaction term. Robust standard errors provided in parenthesis.

across alternative measures of monetary surprises. However, it should be noted that these results tend to be statistically indistinguishable from zero in the second and third specifications. Thus, the evidence for state-dependence largely captures that the conditional effect of monetary surprises on long-dated real forwards was amplified during the financial crisis.

The last column of Table 14 instead uses as the state variable our balance sheet-based measure of arbitrageur duration using the Financial Account and Form PF data described in section 4.2.1.[71] This state variable is measured only quarterly and from Q4 2012 onwards (given the availability of the Form PF data), and almost surely understates the volatility in arbitrageurs' duration as discussed in appendix B.5. As a

[71]We use the measure of duration inclusive of equities. Similar results are obtained using duration in fixed income alone.

result, it is not surprising that we do not find evidence of state-dependence using this variable. This underscores the value of using the price-based measures above.

Proof of Proposition 3. Arbitrageurs' optimality condition for the synthetic dollar bond is

$$\exp(r_t^*) - \exp(r_t) = \text{sign}(X_t^*)\lambda_t,$$

where $\lambda_t \geq 0$ is the multiplier on (30).

Now suppose the constraint is binding and the multiplier $\lambda_t > 0$. If $X_t^* > 0$, the above optimality condition implies that $r_t - r_t^* < 0$. Then given the state variables $\{r_t, \theta_t, \theta_t^*, W_t\}$, $\{X_t^*, Z_t^*, r_t^*\}$ solve

$$\begin{aligned} X_t^* &= \kappa^* W_t, \\ X_t^* + Z_t^* &= 0, \\ Z_t^* &= \alpha^* r_t^* - \theta_t^*. \end{aligned}$$

Straightforward algebra implies

$$r_t^* = \frac{1}{\alpha^*}\left[-\kappa^* W_t + \theta_t^*\right].$$

It follows that a decline in arbitrageur wealth will raise the yield on synthetic dollar bonds and thus make the CIP deviation $r_t - r_t^*$ more negative.

If instead $X_t^* < 0$, the above optimality condition implies that $r_t - r_t^* > 0$. Then $\{X_t^*, Z_t^*, r_t^*\}$ solve

$$\begin{aligned} -X_t^* &= \kappa^* W_t, \\ X_t^* + Z_t^* &= 0, \\ Z_t^* &= \alpha^* r_t^* - \theta_t^*, \end{aligned}$$

which imply

$$r_t^* = \frac{1}{\alpha^*}\left[\kappa^* W_t + \theta_t^*\right].$$

Hence, a decline in arbitrageur wealth will now lower the yield on synthetic dollar bonds and thus make the CIP deviation $r_t - r_t^*$ more positive. □

C Quantitative appendix

We now provide supplementary results for our quantitative analysis in section 5.

C.1 Arbitrageurs' optimality

We first characterize arbitrageurs' optimality conditions in the full model.

Given an equilibrium pricing function

$$P_t^{(\tau)} = P^{(\tau)}(\omega_{1,t}, \omega_{2,t}, W_t),$$

Ito's Lemma implies

$$dP_t^{(\tau)} = \mu_t^{(\tau)} P_t^{(\tau)} dt + \eta_{1,t}^{(\tau)} P_t^{(\tau)} dB_{1,t} + \eta_{2,t}^{(\tau)} P_t^{(\tau)} dB_{2,t} \tag{31}$$

for some coefficients $\mu_t^{(\tau)}$, $\eta_{1,t}^{(\tau)}$, and $\eta_{2,t}^{(\tau)}$ which we have expressed relative to $P_t^{(\tau)}$ without loss of generality, and which we denote with t subscripts as shorthand for these being functions of $(\omega_{1,t}, \omega_{2,t}, W_t)$ as well. Defining the portfolio shares

$$\chi_t^{(\tau)} \equiv \frac{x_t^{(\tau)}}{w_t},$$

we can thus write the arbitrageur problem (3)-(4) as maximizing

$$v(\omega_{1,t}, \omega_{2,t}, W_t, w_t) = \max_{\{\{\chi_{t+s}^{(\tau)}\}\}} E_t \int_0^\infty \exp(-(\xi+\rho)s)(\xi+\rho) \left(\frac{w_{t+s}^{1-\gamma} - 1}{1-\gamma} \right) ds$$

subject to

$$dw_t = \left[w_t r_t + \int_0^\infty \chi_t^{(\tau)} w_t \left(\mu_t^{(\tau)} - r_t \right) d\tau \right] dt + \left[\int_0^\infty \chi_t^{(\tau)} w_t \eta_{1,t}^{(\tau)} d\tau \right] dB_{1,t} + \left[\int_0^\infty \chi_t^{(\tau)} w_t \eta_{2,t}^{(\tau)} d\tau \right] dB_{2,t},$$

and the evolution of aggregates (6)-(9) and (24).

The associated Hamilton-Jacobi-Bellman equation is

$$(\xi+\rho) v_t = -\kappa_1 \omega_{1,t} v_{1,t} - \kappa_2 \omega_{2,t} v_{2,t} + \mu_{W,t} v_{W,t}$$

$$
\begin{aligned}
&+\frac{1}{2}v_{11,t}+\frac{1}{2}v_{22,t}+\frac{1}{2}\left(\eta_{1,t}^{2}+\eta_{2,t}^{2}\right)v_{WW,t}+\eta_{1,t}v_{W1,t}+\eta_{2,t}v_{W2,t}\\
&+\max_{\{\chi_t^{(\tau)}\}}(\xi+\rho)\left(\frac{w_t^{1-\gamma}-1}{1-\gamma}\right)+\left[w_t r_t+\int_0^{\infty}\chi_t^{(\tau)}w_t\left(\mu_t^{(\tau)}-r_t\right)d\tau\right]v_{w,t}\\
&+\frac{1}{2}\left(\left[\int_0^{\infty}\chi_t^{(\tau)}w_t\eta_{1,t}^{(\tau)}d\tau\right]^2+\left[\int_0^{\infty}\chi_t^{(\tau)}w_t\eta_{2,t}^{(\tau)}d\tau\right]^2\right)v_{ww,t}\\
&+\left[\int_0^{\infty}\chi_t^{(\tau)}w_t\eta_{1,t}^{(\tau)}d\tau\right]\left[v_{w1,t}+\eta_{1,t}v_{wW,t}\right]\\
&+\left[\int_0^{\infty}\chi_t^{(\tau)}w_t\eta_{2,t}^{(\tau)}d\tau\right]\left[v_{w2,t}+\eta_{2,t}v_{wW,t}\right], \quad (32)
\end{aligned}
$$

where we write $v_{1,t}$ and $v_{11,t}$ to denote the first- and second-order partial derivatives of $v(\omega_{1,t},\omega_{2,t},W_t,w_t)$ with respect to $\omega_{1,t}$, and analogously for the other first- and second-order partial derivatives. The first-order conditions are

$$
\begin{aligned}
w_t\left(\mu_t^{(\tau)}-r_t\right)v_{w,t}=-w_t^2\left(\int_0^{\infty}\chi_t^{(s)}\left[\eta_{1,t}^{(\tau)}\eta_{1,t}^{(s)}ds+\eta_{2,t}^{(\tau)}\eta_{2,t}^{(s)}\right]ds\right)v_{ww,t}\\
-w_t\eta_{1,t}^{(\tau)}\left[v_{w1,t}+\eta_{1,t}v_{wW,t}\right]-w_t\eta_{2,t}^{(\tau)}\left[v_{w2,t}+\eta_{2,t}v_{wW,t}\right] \quad (33)
\end{aligned}
$$

for each $\tau\in(0,\infty)$.

Now conjecture that the value function satisfies

$$
v(\omega_{1,t},\omega_{2,t},W_t,w_t)=\frac{(\nu_t w_t)^{1-\gamma}-1}{1-\gamma}, \quad (34)
$$

where ν_t does not depend on the arbitrageur's level of wealth, and the t subscript again denotes that it is a function of $(\omega_{1,t},\omega_{2,t},W_t)$. It follows that

$$
\begin{aligned}
v_{w,t}&=\nu_t^{1-\gamma}w_t^{-\gamma},\\
v_{ww,t}&=-\gamma\nu_t^{1-\gamma}w_t^{-\gamma-1},\\
v_{w1,t}&=(1-\gamma)\nu_t^{1-\gamma}w_t^{-\gamma}\frac{\nu_{1,t}}{\nu_t},\\
v_{w2,t}&=(1-\gamma)\nu_t^{1-\gamma}w_t^{-\gamma}\frac{\nu_{2,t}}{\nu_t},\\
v_{wW,t}&=(1-\gamma)\nu_t^{1-\gamma}w_t^{-\gamma}\frac{\nu_{W,t}}{\nu_t}.
\end{aligned}
$$

Substituting into (33), it follows

$$\mu_t^{(\tau)} - r_t = \gamma \int_0^\infty \chi_t^{(s)} \left[\eta_{1,t}^{(\tau)} \eta_{1,t}^{(s)} ds + \eta_{2,t}^{(\tau)} \eta_{2,t}^{(s)} \right] ds$$
$$- (1-\gamma) \eta_{1,t}^{(\tau)} \left[\frac{\nu_{1,t}}{\nu_t} + \eta_{1,t} \frac{\nu_{W,t}}{\nu_t} \right]$$
$$- (1-\gamma) \eta_{2,t}^{(\tau)} \left[\frac{\nu_{2,t}}{\nu_t} + \eta_{2,t} \frac{\nu_{W,t}}{\nu_t} \right] \quad (35)$$

for each $\tau \in (0, \infty)$. An implication is that the arbitrageur's optimal portfolio shares $\chi_t^{(\tau)}$ do not depend on w_t. Substituting these into (32), on the left-hand side we have

$$(\xi + \rho) \frac{(\nu_t w_t)^{1-\gamma} - 1}{1-\gamma}.$$

On the right-hand side, using

$$\begin{aligned}
v_{1,t} &= \nu_t^{1-\gamma} w_t^{1-\gamma} \frac{\nu_{1,t}}{\nu_t}, \\
v_{11,t} &= \nu_t^{1-\gamma} w_t^{1-\gamma} \left(-\gamma \left(\frac{\nu_{1,t}}{\nu_t} \right)^2 + \frac{\nu_{11,t}}{\nu_t} \right), \\
v_{2,t} &= \nu_t^{1-\gamma} w_t^{1-\gamma} \frac{\nu_{2,t}}{\nu_t}, \\
v_{22,t} &= \nu_t^{1-\gamma} w_t^{1-\gamma} \left(-\gamma \left(\frac{\nu_{2,t}}{\nu_t} \right)^2 + \frac{\nu_{22,t}}{\nu_t} \right), \\
v_{W,t} &= \nu_t^{1-\gamma} w_t^{1-\gamma} \frac{\nu_{W,t}}{\nu_t}, \\
v_{WW,t} &= \nu_t^{1-\gamma} w_t^{1-\gamma} \left(-\gamma \left(\frac{\nu_{W,t}}{\nu_t} \right)^2 + \frac{\nu_{WW,t}}{\nu_t} \right), \\
v_{W1,t} &= \nu_t^{1-\gamma} w_t^{1-\gamma} \left(-\gamma \frac{\nu_{W,t}}{\nu_t} \frac{\nu_{1,t}}{\nu_t} + \frac{\nu_{W1,t}}{\nu_t} \right), \\
v_{W2,t} &= \nu_t^{1-\gamma} w_t^{1-\gamma} \left(-\gamma \frac{\nu_{W,t}}{\nu_t} \frac{\nu_{2,t}}{\nu_t} + \frac{\nu_{W2,t}}{\nu_t} \right),
\end{aligned}$$

we have

$$\nu_t^{1-\gamma} w_t^{1-\gamma} \Bigg[- \kappa_1 \omega_{1,t} \frac{\nu_{1,t}}{\nu_t} - \kappa_2 \omega_{2,t} \frac{\nu_{2,t}}{\nu_t} + \mu_{W,t} \frac{\nu_{W,t}}{\nu_t}$$
$$+ \frac{1}{2} \left(-\gamma \left(\frac{\nu_{1,t}}{\nu_t} \right)^2 + \frac{\nu_{11,t}}{\nu_t} \right) + \frac{1}{2} \left(-\gamma \left(\frac{\nu_{2,t}}{\nu_t} \right)^2 + \frac{\nu_{22,t}}{\nu_t} \right)$$

$$
\begin{aligned}
&+\frac{1}{2}\left(\eta_{1,t}^2+\eta_{2,t}^2\right)\left(-\gamma\left(\frac{\nu_{W,t}}{\nu_t}\right)^2+\frac{\nu_{WW,t}}{\nu_t}\right)\\
&+\eta_{1,t}\left(-\gamma\frac{\nu_{W,t}}{\nu_t}\frac{\nu_{1,t}}{\nu_t}+\frac{\nu_{W1,t}}{\nu_t}\right)+\eta_{2,t}\left(-\gamma\frac{\nu_{W,t}}{\nu_t}\frac{\nu_{2,t}}{\nu_t}+\frac{\nu_{W2,t}}{\nu_t}\right)\\
&+\left[r_t+\int_0^\infty\chi_t^{(\tau)}\left(\mu_t^{(\tau)}-r_t\right)d\tau\right]\\
&-\frac{1}{2}\gamma\left(\left[\int_0^\infty\chi_t^{(\tau)}\eta_{1,t}^{(\tau)}d\tau\right]^2+\left[\int_0^\infty\chi_t^{(\tau)}\eta_{2,t}^{(\tau)}d\tau\right]^2\right)\\
&+(1-\gamma)\left[\int_0^\infty\chi_t^{(\tau)}\eta_{1,t}^{(\tau)}d\tau\right]\left[\frac{\nu_{1,t}}{\nu_t}+\eta_{1,t}\frac{\nu_{W,t}}{\nu_t}\right]\\
&+(1-\gamma)\left[\int_0^\infty\chi_t^{(\tau)}\eta_{2,t}^{(\tau)}d\tau\right]\left[\frac{\nu_{2,t}}{\nu_t}+\eta_{2,t}\frac{\nu_{W,t}}{\nu_t}\right]\Bigg]+(\xi+\rho)\frac{w_t^{1-\gamma}-1}{1-\gamma}.
\end{aligned}
$$

Subtracting $(\xi+\rho)\frac{w_t^{1-\gamma}-1}{1-\gamma}$ from both sides and dividing by $w_t^{1-\gamma}$, (32) becomes

$$
\begin{aligned}
(\xi+\rho)\frac{\nu_t^{1-\gamma}-1}{1-\gamma}=\nu_t^{1-\gamma}\Bigg[&-\kappa_1\omega_{1,t}\frac{\nu_{1,t}}{\nu_t}-\kappa_2\omega_{2,t}\frac{\nu_{2,t}}{\nu_t}+\mu_{W,t}\frac{\nu_{W,t}}{\nu_t}\\
&+\frac{1}{2}\left(-\gamma\left(\frac{\nu_{1,t}}{\nu_t}\right)^2+\frac{\nu_{11,t}}{\nu_t}\right)+\frac{1}{2}\left(-\gamma\left(\frac{\nu_{2,t}}{\nu_t}\right)^2+\frac{\nu_{22,t}}{\nu_t}\right)\\
&+\frac{1}{2}\left(\eta_{1,t}^2+\eta_{2,t}^2\right)\left(-\gamma\left(\frac{\nu_{W,t}}{\nu_t}\right)^2+\frac{\nu_{WW,t}}{\nu_t}\right)\\
&+\eta_{1,t}\left(-\gamma\frac{\nu_{W,t}}{\nu_t}\frac{\nu_{1,t}}{\nu_t}+\frac{\nu_{W1,t}}{\nu_t}\right)+\eta_{2,t}\left(-\gamma\frac{\nu_{W,t}}{\nu_t}\frac{\nu_{2,t}}{\nu_t}+\frac{\nu_{W2,t}}{\nu_t}\right)\\
&+\left[r_t+\int_0^\infty\chi_t^{(\tau)}\left(\mu_t^{(\tau)}-r_t\right)d\tau\right]\\
&-\frac{1}{2}\gamma\left(\left[\int_0^\infty\chi_t^{(\tau)}\eta_{1,t}^{(\tau)}d\tau\right]^2+\left[\int_0^\infty\chi_t^{(\tau)}\eta_{2,t}^{(\tau)}d\tau\right]^2\right)\\
&+(1-\gamma)\left[\int_0^\infty\chi_t^{(\tau)}\eta_{1,t}^{(\tau)}d\tau\right]\left[\frac{\nu_{1,t}}{\nu_t}+\eta_{1,t}\frac{\nu_{W,t}}{\nu_t}\right]\\
&+(1-\gamma)\left[\int_0^\infty\chi_t^{(\tau)}\eta_{2,t}^{(\tau)}d\tau\right]\left[\frac{\nu_{2,t}}{\nu_t}+\eta_{2,t}\frac{\nu_{W,t}}{\nu_t}\right]\Bigg]. \quad (36)
\end{aligned}
$$

Since nothing in this partial differential equation depends on w_t, the conjectured form of the value function is satisfied, with ν_t solving the above equation.

Finally, since $\chi_t^{(\tau)}$ does not depend on arbitrageurs' individual wealth, aggregation implies

$$\chi_t^{(\tau)} = \frac{X_t^{(\tau)}}{W_t},$$

so that (35) can be written

$$\mu_t^{(\tau)} - r_t = \frac{\gamma}{W_t}\int_0^\infty X_t^{(s)}\left[\eta_{1,t}^{(\tau)}\eta_{1,t}^{(s)}ds + \eta_{2,t}^{(\tau)}\eta_{2,t}^{(s)}\right]ds \\ - (1-\gamma)\left[\eta_{1,t}^{(\tau)}\frac{\nu_{1,t}}{\nu_t} + \eta_{2,t}^{(\tau)}\frac{\nu_{2,t}}{\nu_t} + \left(\eta_{1,t}^{(\tau)}\eta_{1,t} + \eta_{2,t}^{(\tau)}\eta_{2,t}\right)\frac{\nu_{W,t}}{\nu_t}\right]. \quad (37)$$

Given (31) together with

$$d\nu_t = \Bigg[- \kappa_1\omega_{1,t}\nu_{1,t} - \kappa_2\omega_{2,t}\nu_{2,t} + \mu_{W,t}\nu_{W,t} + \frac{1}{2}\nu_{11,t} + \frac{1}{2}\nu_{22,t} + \frac{1}{2}\left(\eta_{1,t}^2 + \eta_{2,t}^2\right)\nu_{WW,t} \\ + \eta_{1,t}\nu_{W1,t} + \eta_{2,t}\nu_{W2,t}\Bigg]dt + \left(\nu_{1,t} + \eta_{1,t}\nu_{W,t}\right)dB_{1,t} + \left(\nu_{2,t} + \eta_{2,t}\nu_{W,t}\right)dB_{2,t},$$

which follows from Ito's Lemma, (37) can be more intuitively written

$$E_t\left(\frac{dP_t^{(\tau)}}{P_t^{(\tau)}}\right) - r_t dt = \\ \frac{\gamma}{W_t}\int_0^\infty X_t^{(s)} Cov_t\left(\frac{dP_t^{(\tau)}}{P_t^{(\tau)}}, \frac{dP_t^{(s)}}{P_t^{(s)}}\right)ds - (1-\gamma)Cov\left(\frac{dP_t^{(\tau)}}{P_t^{(\tau)}}, \frac{d\nu_t}{\nu_t}\right)$$

as in the main text. As described in the main text, this generalizes the expression for expected excess returns in Vayanos and Vila (2021) in two ways. First, owing to CRRA preferences, W_t appears in the denominator of the first term on the right-hand side. Second, when $\gamma \neq 1$, arbitrageurs have a standard intertemporal hedging motive that also affects expected excess returns. In particular, arbitrageurs require a lower excess return on a bond of maturity τ if it pays well when $(1-\gamma)d\nu_t$ and thus the (instantaneously future) marginal utility of wealth is high. The latter motive is eliminated when $\gamma = 1$ (log preferences). It is also eliminated when $\rho \to \infty$, in which case $\nu_t = 1$ solves the partial differential equation (36). We focus on the latter case and later in this appendix consider the case with general ρ.

C.2 Solution algorithm

We now provide more details on our computational algorithm.

Algorithm Given (8), (9), (23), and (24), Ito's Lemma and $d\tau = -dt$ implies that

$$\begin{aligned}\frac{dP_t^{(\tau)}}{P_t^{(\tau)}} = \frac{1}{P_t^{(\tau)}} \Big[& -P_{1,t}^{(\tau)}\kappa_1\omega_{1,t} - P_{2,t}^{(\tau)}\kappa_2\omega_{2,t} + P_{W,t}^{(\tau)}\mu_{W,t} - P_{\tau,t}^{(\tau)} \\ & + \frac{1}{2}P_{11,t}^{(\tau)} + \frac{1}{2}P_{22,t}^{(\tau)} + \frac{1}{2}P_{WW,t}^{(\tau)}\left(\eta_{1,t}^2 + \eta_{2,t}^2\right) + P_{W1,t}^{(\tau)}\eta_{1,t} + P_{W2,t}^{(\tau)}\eta_{2,t} \Big] dt \\ & + \frac{1}{P_t^{(\tau)}}\left(P_{1,t}^{(\tau)} + P_{W,t}^{(\tau)}\eta_{1,t}\right) dB_{1,t} + \frac{1}{P_t^{(\tau)}}\left(P_{2,t}^{(\tau)} + P_{W,t}^{(\tau)}\eta_{2,t}\right) dB_{2,t},\end{aligned}$$

where we again write $P_{x,t}^{(\tau)}$ and $P_{xx,t}^{(\tau)}$ to denote the first- and second-order partial derivatives of $P^{(\tau)}(\omega_{1,t}, \omega_{2,t}, W_t)$, and we again write $\mu_{W,t} = \mu_W(\omega_{1,t}, \omega_{2,t}, W_t)$ and analogously for $\eta_{1,t}$ and $\eta_{2,t}$. It follows that

$$\begin{aligned}E_t\left(dP_t^{(\tau)}\right) = \Big[& -P_{1,t}^{(\tau)}\kappa_1\omega_{1,t} - P_{2,t}^{(\tau)}\kappa_2\omega_{2,t} + P_{W,t}^{(\tau)}\mu_{W,t} - P_{\tau,t}^{(\tau)} \\ & + \frac{1}{2}P_{11,t}^{(\tau)} + \frac{1}{2}P_{22,t}^{(\tau)} + \frac{1}{2}P_{WW,t}^{(\tau)}\left(\eta_{1,t}^2 + \eta_{2,t}^2\right) + P_{W1,t}^{(\tau)}\eta_{1,t} + P_{W2,t}^{(\tau)}\eta_{2,t} \Big] dt\end{aligned}$$

and

$$\begin{aligned}Cov_t\left(dP_t^{(\tau)}, dP_t^{(s)}\right) = & \left(P_{1,t}^{(\tau)} + P_{W,t}^{(\tau)}\eta_{1,t}\right)\left(P_{1,t}^{(s)} + P_{W,t}^{(s)}\eta_{1,t}\right) dt \\ & + \left(P_{2,t}^{(\tau)} + P_{W,t}^{(\tau)}\eta_{2,t}\right)\left(P_{2,t}^{(s)} + P_{W,t}^{(s)}\eta_{2,t}\right) dt.\end{aligned}$$

Plugging both into (21), we obtain the partial differential equation

$$\begin{aligned}& \Big[-P_{1,t}^{(\tau)}\kappa_1\omega_{1,t} - P_{2,t}^{(\tau)}\kappa_2\omega_{2,t} + P_{W,t}^{(\tau)}\mu_{W,t} - P_{\tau,t}^{(\tau)} \\ & + \frac{1}{2}P_{11,t}^{(\tau)} + \frac{1}{2}P_{22,t}^{(\tau)} + \frac{1}{2}P_{WW,t}^{(\tau)}\left(\eta_{1,t}^2 + \eta_{2,t}^2\right) + P_{W1,t}^{(\tau)}\eta_{1,t} + P_{W2,t}^{(\tau)}\eta_{2,t} - r_t P_t^{(\tau)} \Big] dt \\ & = \frac{\gamma}{W_t}\Bigg[\left(P_{1,t}^{(\tau)} + P_{W,t}^{(\tau)}\eta_{1,t}\right)\int_0^\infty \left(\alpha(s)\log\left(P_t^{(s)}\right) + \theta_0(s) + \theta_1(s)\beta_t\right)\frac{1}{P_t^{(s)}}\left(P_{1,t}^{(s)} + P_{W,t}^{(s)}\eta_{1,t}\right) ds \\ & + \left(P_{2,t}^{(\tau)} + P_{W,t}^{(\tau)}\eta_{2,t}\right)\int_0^\infty \left(\alpha(s)\log\left(P_t^{(s)}\right) + \theta_0(s) + \theta_1(s)\beta_t\right)\frac{1}{P_t^{(s)}}\left(P_{2,t}^{(s)} + P_{W,t}^{(s)}\eta_{2,t}\right) ds \Bigg] dt.\end{aligned}$$

Collecting terms, this can be written

$$P_{1,t}^{(\tau)}\mu_{1,t}^{Q} + P_{2,t}^{(\tau)}\mu_{2,t}^{Q} + P_{W,t}^{(\tau)}\mu_{W,t}^{Q} - P_{\tau,t}^{(\tau)} - r_t P_t^{(\tau)} \tag{38}$$
$$+ \frac{1}{2}P_{11,t}^{(\tau)} + \frac{1}{2}P_{22,t}^{(\tau)} + \frac{1}{2}P_{WW,t}^{(\tau)}\left(\eta_{1,t}^2 + \eta_{2,t}^2\right) + P_{W1,t}^{(\tau)}\eta_{1,t} + P_{W2,t}^{(\tau)}\eta_{2,t} = 0,$$

where

$$\mu_{1,t}^{Q} = -\kappa_1\omega_{1,t} - \frac{\gamma}{W_t}\eta_{1,t}, \tag{39}$$

$$\mu_{2,t}^{Q} = -\kappa_2\omega_{2,t} - \frac{\gamma}{W_t}\eta_{2,t}, \tag{40}$$

$$\mu_{W,t}^{Q} = \mu_{W,t} - \frac{\gamma}{W_t}\Big(\eta_{1,t}^2 + \eta_{2,t}^2\Big), \tag{41}$$

where the notation anticipates that these are the drifts of the state variables under the risk neutral measure Q, and we also anticipate the expressions for $\eta_{1,t}$ and $\eta_{2,t}$ in (47) and (48) below.

Using the Feynman-Kac formula, the solution to a PDE of the form (38) is

$$P_t^{(\tau)} = E_t^{Q}\left[e^{-\int_0^\tau r_{t+s}ds}\right], \tag{42}$$

where the stochastic processes of $\omega_{1,t}$, $\omega_{2,t}$ and W_t under Q are given by

$$d\omega_{1,t} = \mu_1^{Q}(\omega_{1,t}, \omega_{2,t}, W_t)dt + dB_{1,t}, \tag{43}$$

$$d\omega_{2,t} = \mu_2^{Q}(\omega_{1,t}, \omega_{2,t}, W_t)dt + dB_{2,t}, \tag{44}$$

$$dW_t = \mu_W^{Q}(\omega_{1,t}, \omega_{2,t}, W_t)dt + \eta_1(\omega_{1,t}, \omega_{2,t}, W_t)dB_{1,t} + \eta_2(\omega_{1,t}, \omega_{2,t}, W_t)dB_{2,t}. \tag{45}$$

Finally, (22), (24), and the method of undetermined coefficients imply

$$\mu_{W,t} = \xi\left(\bar{W} - W_t\right)$$
$$+ W_t r_t + \int_0^\infty \left(\alpha(\tau)\log\left(P_t^{(\tau)}\right) + \theta_0(\tau) + \theta_1(\tau)\beta_t\right)\left(\mu_t^{(\tau)} - r_t\right)d\tau, \tag{46}$$

$$\eta_{1,t} = \int_0^\infty \left(\alpha(\tau)\log\left(P_t^{(\tau)}\right) + \theta_0(\tau) + \theta_1(\tau)\beta_t\right)\frac{1}{P_t^{(\tau)}}\left(P_{1,t}^{(\tau)} + P_{W,t}^{(\tau)}\eta_{1,t}\right)d\tau, \tag{47}$$

$$\eta_{2,t} = \int_0^\infty \left(\alpha(\tau)\log\left(P_t^{(\tau)}\right) + \theta_0(\tau) + \theta_1(\tau)\beta_t\right)\frac{1}{P_t^{(\tau)}}\left(P_{2,t}^{(\tau)} + P_{W,t}^{(\tau)}\eta_{2,t}\right)d\tau, \tag{48}$$

where $\mu_t^{(\tau)}$ is the expected instantaneous return on a bond of maturity τ defined in

(31).

This motivates the following computational algorithm:[72]

1. Create a tensor grid of ω_t, ω_2, and W values.
2. Initialize $\mu_1^Q(\omega_1, \omega_2, W)$, $\mu_2^Q(\omega_1, \omega_2, W)$, $\mu_W^Q(\omega_1, \omega_2, W)$, $\mu_W(\omega_1, \omega_2, W)$, $\eta_1(\omega_1, \omega_2, W)$, and $\eta_2(\omega_1, \omega_2, W)$ at each grid point. In the first iteration, set them to zero.
3. Use cubic splines to approximate $\mu_1^Q(\omega_1, \omega_2, W)$, $\mu_2^Q(\omega_1, \omega_2, W)$, $\mu_W^Q(\omega_1, \omega_2, W)$, $\mu_W(\omega_1, \omega_2, W)$, $\eta_1(\omega_1, \omega_2, W)$, and $\eta_2(\omega_1, \omega_2, W)$ outside of the grid points.
4. Approximate (42) using Monte Carlo simulation:
   (a) For each grid point simulate N sequences of ω_1, ω_2, and W of length $\bar{\tau}/dt$, where dt is the size of the time steps in the simulation. The stochastic processes are approximated using the Euler-Maruyama method.
   (b) Calculate an approximation of the price of a bond of maturity τ at each grid point as

$$P^{(\tau)}(\omega_1, \omega_2, W) = E_t^Q \left[e^{-\int_0^\tau r_{t+s} ds} | (\omega_1, \omega_2, W) \right] \approx \frac{1}{N} \sum_{n=1}^{N} e^{-\sum_{i=1}^{\tau/dt} r_{n,i}(\omega_1, \omega_2, W) dt},$$

   where $r_{n,i}(\omega_1, \omega_2, W)$ denotes the ith observation in the nth simulation of the interest rate process starting from state (ω_1, ω_2, W) at t (using (6)).
5. Update the values for $\mu_1^Q(\omega_1, \omega_2, W)$, $\mu_2^Q(\omega_1, \omega_2, W)$, $\mu_W^Q(\omega_1, \omega_2, W)$, $\mu_W(\omega_1, \omega_2, W)$, $\eta_1(\omega_1, \omega_2, W)$, and $\eta_2(\omega_1, \omega_2, W)$ using (39)-(41) and (46)-(48).
6. If the values in step 5 are sufficiently close to those guessed in step 2, stop. Otherwise, return to step 2 using the values in step 5.

Finally, we note one adjustment we make to the environment to facilitate the solution of the model on wide enough grids for the state variables: we modify the specification of habitat demand (2) so that

$$\theta_t(\tau) = \theta_0(\tau) + \theta_1(\tau) \left(1 - \frac{1}{1 + bW_t} \right) \beta_t,$$

[72] Our code is written in Julia and solves the model in less than 30 minutes on a desktop computer. The code and additional details on the solution algorithm are available on GitHub.

where b is a large scalar. This in turn enters conditions (46)-(48). The factor $1 - \frac{1}{1+bW_t}$ is monotonic in wealth W_t and equals zero at $W_t = 0$ and one at $W_t \to \infty$. It facilitates stability of the numerical solution for wider grids, as it means habitat demand has less volatility when wealth is low (there is no effect on the average level of habitat demand, as β_t has zero mean). We set $b = 3/0.1$, where 0.1 is the center of the wealth grid, so that at the grid center this factor already is 0.75 and is very flat in wealth. We also emphasize that this factor pushes against our model's ability to deliver a rise in the term premium upon a monetary tightening, as it implies that the volatility of demand shocks (slightly) falls when arbitrageurs lose wealth.

Accuracy We can evaluate the accuracy of our numerical algorithm by considering the case with $\xi \to \infty$. With exogenous wealth, there is a closed form solution for the bond price $P^{(\tau)}(\omega_1, \omega_2)$ as derived in Vayanos and Vila (2021).[73,74] Table 15 compares the numerical and closed form solutions, using the same parametrization as Vayanos and Vila (2021). We report the same moments as in Table 1 in that paper. As is evident, the first and second moments of the numerical solution are very close to those from the closed form solution. The same conclusion holds for the entire yield curve at least over the support of state variables over which the numerical grid is defined, which extends 3 to 5 standard deviations in each variable in each direction.

Equilibrium existence and selection We finally comment on equilibrium existence and the equilibrium selected by our algorithm when there are multiple equilibria.

In existing preferred habitat models without endogenous wealth, equilibrium existence depends on parameter values. In particular, Greenwood and Vayanos (2014)

[73] In particular, (6)-(9) and Ito's Lemma imply

$$dr_t = -\sigma_{r,1}\kappa_1\omega_{1,t} - \sigma_{r,2}\kappa_2\omega_{2,t} + \sigma_{r,1}dB_{1,t} + \sigma_{r,2}dB_{2,t},$$
$$d\beta_t = -\sigma_{\beta,1}\kappa_1\omega_{1,t} - \sigma_{\beta,2}\kappa_2\omega_{2,t} + \sigma_{\beta,1}dB_{1,t} + \sigma_{\beta,2}dB_{2,t}.$$

Given (6) and (7), we have

$$\omega_{1,t} = -\frac{\sigma_{\beta,2}}{\sigma_{\beta,1}\sigma_{r,2} - \sigma_{r,1}\sigma_{\beta,2}}(r_t - \bar{r}) + \frac{\sigma_{r,2}}{\sigma_{\beta,1}\sigma_{r,2} - \sigma_{r,1}\sigma_{\beta,2}}\beta_t,$$
$$\omega_{2,t} = \frac{\sigma_{\beta,1}}{\sigma_{\beta,1}\sigma_{r,2} - \sigma_{r,1}\sigma_{\beta,2}}(r_t - \bar{r}) - \frac{\sigma_{r,1}}{\sigma_{\beta,1}\sigma_{r,2} - \sigma_{r,1}\sigma_{\beta,2}}\beta_t.$$

Combining these implies the evolution of r_t and β_t directly in terms of the Wiener increments. It is then straightforward to apply the solution approach in Vayanos and Vila (2021).

[74] The factor described in the prior paragraph does not change the fact that the model nests Vayanos and Vila (2021) when $\xi \to \infty$, since of course in that case $1 - \frac{1}{1+bW_t} = 1 - \frac{1}{1+b\bar{W}}$ is simply a constant.

Moment	Numerical	Closed form
$\sigma(y_t^{(1)})$	2.61%	2.62%
$\sigma(\Delta y_t^{(1)})$	1.28%	1.27%
$\frac{1}{30}\sum_{\tau=1}^{30}\sigma(y_t^{(\tau)})$	2.13%	2.20%
$\frac{1}{30}\sum_{\tau=1}^{30}\sigma(\Delta y_t^{(\tau)})$	0.806	0.796
$\frac{1}{30}\sum_{\tau=1}^{30}\rho(\Delta y_t^{1}, \Delta y_t^{(\tau)})$	0.506	0.504

Table 15: numerical solution versus closed form solution from Vayanos and Vila (2021)

Notes: parameters are as described in Table 1 of Vayanos and Vila (2021).

demonstrate that an affine equilibrium in state variables does not exist if arbitrageur risk aversion is sufficiently high (see their Theorem 1). While the equilibrium is not affine in the case with endogenous wealth, simulations suggest that a similar restriction on existence holds in this setting. In particular, our numerical algorithm does not converge for sufficiently high levels of risk aversion.

In models without endogenous wealth, there are also multiple equilibria when an equilibrium exists, as the price impact of demand shocks is self-fulfilling (see again Theorem 1 of Greenwood and Vayanos (2014)). As risk aversion approaches zero, only one of these equilibria converges to the unique equilibrium that obtains with risk neutral arbitrageurs, namely the (local) expectations hypothesis. While we do not have a proof that the environment with endogenous wealth also features multiplicity, the same intuition as in the exogenous wealth case suggests that it will. However, we believe our solution algorithm quite robustly selects the equilibrium with well-behaved convergence properties, for two reasons.

First, in the solution algorithm, we initialize the drifts and loadings of state variables under the risk neutral measure to those that would indeed be obtained with risk neutrality, and we slowly update these drifts and loadings until we have converged to an equilibrium. Hence, it is natural that the algorithm will select the equilibrium which converges to the local expectations hypothesis when $\gamma = 0$.

Second, our equilibrium pricing function indeed evolves continuously in γ, approaching the local expectations hypothesis. Figure 14 plots the yield curve obtained using our solution algorithm for $\omega_{1,t} = 0$, $\omega_{2,t} = 0$, and $W_t = \bar{W}$. Starting with our baseline calibration, the yield curve converges smoothly to that under the local expectations hypothesis as we lower γ to approach a calibration with risk neutral arbitrageurs.

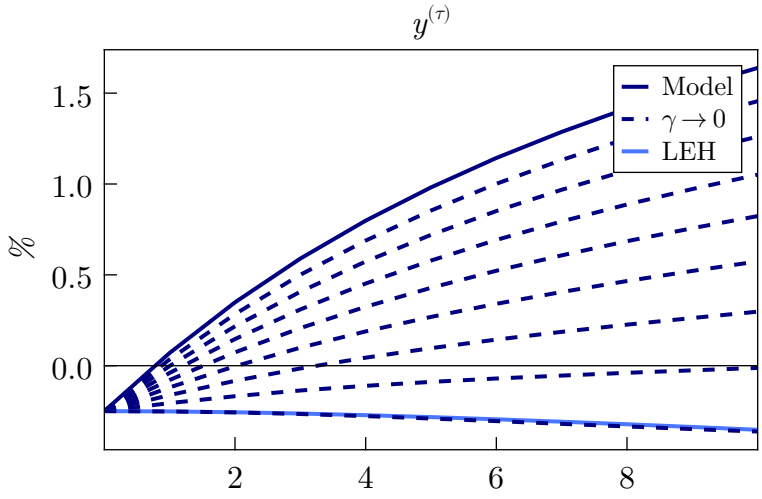

Figure 14: convergence of equilibrium to local expectations hypothesis

Notes: equilibrium yield curve depicted for fixed state variables: $\omega_{1,t} = 0$, $\omega_{2,t} = 0$, and $W_t = \bar{W}$. "LEH" denotes local expectations hypothesis, given by $y^{(\tau)} = \bar{r} + \frac{\sigma_{1r}^2}{2\kappa_1^2}\left(\frac{B_1(\tau)-\tau}{\tau}\right) + \frac{\sigma_{1r}^2}{4\kappa_1}\frac{B_1(\tau)^2}{\tau} + \frac{\sigma_{2r}^2}{2\kappa_2^2}\left(\frac{B_2(\tau)-\tau}{\tau}\right) + \frac{\sigma_{2r}^2}{4\kappa_2}\frac{B_2(\tau)^2}{\tau}$, where $B_1(\tau) = \frac{1-e^{-\kappa_1\tau}}{\kappa_1}$ and $B_2(\tau) = \frac{1-e^{-\kappa_2\tau}}{\kappa_2}$, applying Vasicek (1977) to the present environment with two components of the short rate.

C.3 Decomposing the forward rate responses

We can use the following decomposition to understand more deeply why long-dated real forwards rise upon a monetary tightening in the model. Following Cochrane and Piazzesi (2008), standard identities imply that

$$f_t^{(\tau-1,\tau)} - y_{t+\tau-1}^{(1)} = \left[r_{t+1}^{(\tau)} - r_{t+1}^{(\tau-1)}\right] + \left[r_{t+2}^{(\tau-1)} - r_{t+2}^{(\tau-2)}\right] + \ldots + \left[r_{t+\tau-1}^{(2)} - y_{t+\tau-2}^{(1)}\right], \quad (49)$$

where $r_{t+1}^{(\tau)}$ denotes the log return to purchasing a τ-period bond at t and holding it for one year:

$$r_{t+1}^{(\tau)} \equiv \log P_{t+1}^{(\tau-1)} - \log P_t^{(\tau)}.$$

The left-hand side of (49) is the forward-spot spread. The right-hand side of (49) reflects the cumulative return to a sequence of carry strategies: purchasing a (τ)-year bond at t financed by a $(\tau-1)$-year bond, then purchasing a $(\tau-1)$-year bond at $t+1$ financed by a $(\tau-2)$-year bond, and so on. Evaluating this identity ex-ante instead of ex-post and taking expectations at t, we have that

$$f_t^{(\tau-1,\tau)} - E_t y_{t+\tau-1}^{(1)} =$$

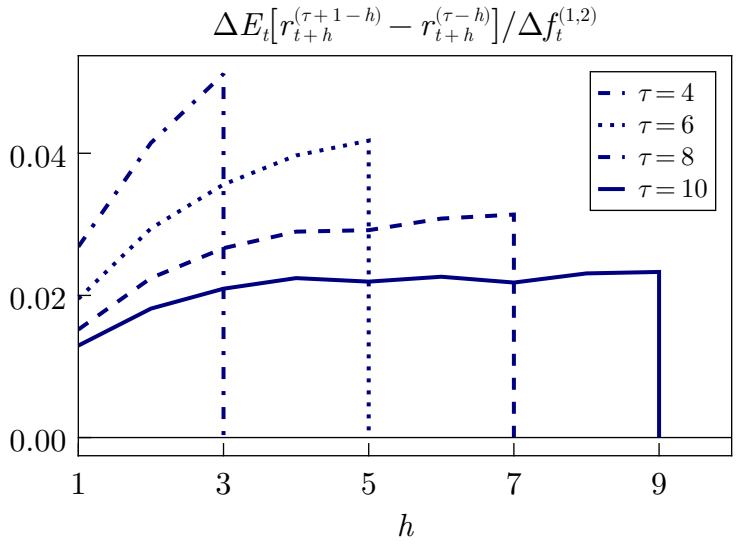

Figure 15: decomposing $\Delta[f_t^{(\tau-1,\tau)} - E_t y_{t+\tau-1}^{(1)}]/\Delta f_t^{(1,2)}$ on impact of monetary shock

Notes: as derived in (50), $f_t^{(\tau-1,\tau)} - E_t y_{t+\tau-1}^{(1)} = \sum_{h=1}^{\tau-1} E_t \left[r_{t+h}^{(\tau+1-h)} - r_{t+h}^{(\tau-h)} \right]$. Responses simulated as described in Figure 2.

$$E_t \left[r_{t+1}^{(\tau)} - r_{t+1}^{(\tau-1)} \right] + E_t \left[r_{t+2}^{(\tau-1)} - r_{t+2}^{(\tau-2)} \right] + \ldots + E_t \left[r_{t+\tau-1}^{(2)} - y_{t+\tau-2}^{(1)} \right]. \quad (50)$$

It follows that the response of the forward rate relative to the expected spot rate — the difference between the relevant lines in Figure 3 — encodes the response of expected excess returns on a sequence of carry trades at future dates.

Figure 15 depicts the response of each of these expected excess returns for $\tau = \{4, 6, 8, 10\}$-year bonds corresponding to the baseline results in Figure 3. At $h = 1$ (the first year after the monetary tightening), we see that the initial increase in expected carry trade returns is highest for four-year bonds, then six-year bonds, and so on. This reflects the fact that average carry trade returns are themselves falling in maturity: 10- and nine-year bonds do not have much different sensitivities to aggregate risk factors, whereas five- and four-year bonds do. However, because longer dated forward rates encode the response of expected carry trade returns over a longer horizon h, the difference in forward rates $f_t^{(\tau-1,\tau)}$ and expected spot rates $E_t y_{t+\tau-1}^{(1)}$ rises in τ, even though the initial response in carry trade returns is smaller for bonds with higher τ.

Thus, the model rationalizes the response of long-dated forward rates to a monetary shock through a persistent change in risk premia following the shock.

C.4 QE in data and model

QE in the model is a habitat demand shock, since we calibrate the model so that the Federal Reserve is among the set of habitat investors. In this appendix we provide the evidence on QE and the mapping between model and data used in calibration.

C.4.1 QE in data

We first describe the evidence on QE, building on a large literature. We focus on the first round of QE from November 2008 through March 2010, and measure both the Federal Reserve's purchases as well as the announcement effects on the yield curve.

Purchases The first round of QE consisted of purchases of Treasuries, agency/GSE-backed debt securities, and mortgage-backed securities (MBS). We measure the purchases of Treasuries and agency/GSE-backed debt securities from the System Open Market Account (SOMA) Holdings of Domestic Securities reported by the Federal Reserve Bank of New York.[75] We measure the purchases of MBS from the transaction-level data for the Agency Mortgage-Backed Securities Purchase Program organized by the Federal Reserve Board. All purchases are at the CUSIP level.

We then transform these purchases into a panel dataset of purchases of zero coupon bonds purchased at each maturity $\tau \in (0, 30]$ on each date t. For Treasuries and agency/GSE-backed debt securities, we observe each security's coupon, term, and par value purchased. We thus strip the security into its constituent payments at each future date and compute the market values of each stripped payment using the daily nominal yield curve estimated by Gurkaynak et al. (2006). For MBS, we observe each security's market value purchased. While we also observe the security's coupon and term, these securities have substantial pre-payment risk and thus their effective duration is much shorter than simple duration. For simplicity we thus assume that all MBS purchased on a given date are zero coupon bonds with maturity equal to the effective duration of the Bloomberg MBS index on that date.

Figure 16 summarizes the Federal Reserve's purchases over this period in terms of the equivalent purchase of 10-year zero coupon bonds (in terms of having the same

[75] Since this dataset only provides the par value of holdings by security, we define purchases as the change in the par value from one week to the next. This dataset also does not distinguish between Treasuries purchased as part of QE and Treasuries purchased as part of more standard open market operations. We (largely) isolate the former by focusing only on Treasury purchases after March 18, 2009 of securities with a remaining time to maturity of at least two years.

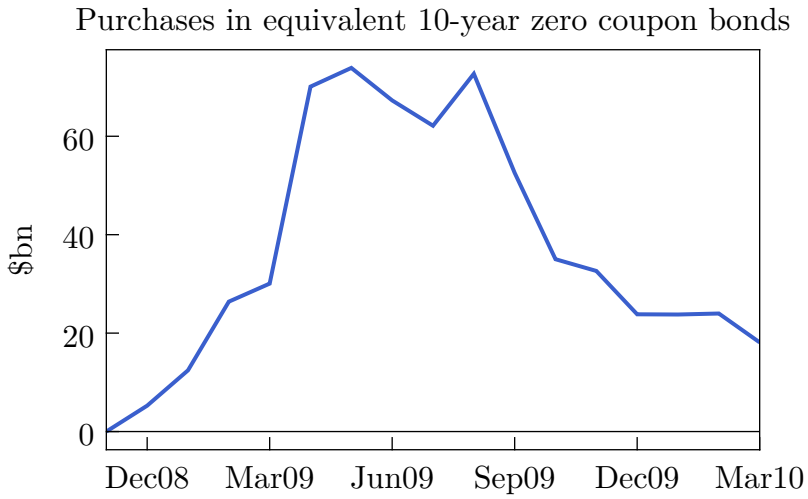

Figure 16: Federal Reserve purchases in first round of QE

Notes: figure depicts amount of 10-year zero coupon bonds equivalent to the total amount of duration purchased by the Federal Reserve in Treasuries, agency/GSE-backed debt securities, and mortgage-backed securities each month.

duration as the securities purchased). We estimate that the cumulative purchases totaled over $600 billion in 10-year equivalent zero coupon bonds, consistent with other estimates in the literature (e.g., Gagnon, Raskin, Remache, and Sack (2011)).

Announcement effects on yield curve We next measure the announcement effects of QE on the TIPS yield curve. We focus on the TIPS yield curve given the paper's maintained focus on the real term structure. Together with the data on purchases, this will allow us to discipline the price elasticities in the model.

Using Gurkaynak et al. (2008)'s interpolated TIPS yield curve (as throughout our analysis), Table 16 summarizes the two-day changes in the five- and 10-year yields and one-year forward rates paying in five and 10 years on each of the announcement days.[76] We refer the reader to Gagnon et al. (2011) for a description of each announcement. We follow Krishnamurthy and Vissing-Jorgensen (2011) in distinguishing the first five announcements from the subsequent three, as the former had larger effects. We find that the cumulative declines in the five- and 10-year TIPS yields on announcement days were 204*bp* and 188*bp*, respectively. The cumulative declines in the forward rates were 238*bp* and 117*bp*. The latter is direct evidence of a compression of risk premiums,

[76]We follow Krishnamurthy and Vissing-Jorgensen (2011) in using two-day changes, but similar results are obtained using one-day changes.

	$\Delta y_t^{(5)}$	$\Delta y_t^{(10)}$	$\Delta f_t^{(4,5)}$	$\Delta f_t^{(9,10)}$
11/25/2008	-15	-39	-53	-48
12/1/2008	-47	-34	-53	-10
12/16/2008	-74	-58	-60	-31
1/28/2009	4	9	11	16
3/18/2009	-62	-61	-74	-46
Sum to date	-194	-183	-230	-119
8/12/2009	0	-0	-1	-1
9/23/2009	-2	-1	-2	1
11/4/2009	-8	-3	-5	2
Sum to date	-204	-188	-238	-117

Table 16: announcement effects on real yield curve

Notes: all values in *bp*. Effect computed as the value at the end of the trading day following the announcement day, less the value at the end of the trading day prior to the announcement day.

under the maintained assumption that the announcements contained no news about real interest rates so far into the future.

Our estimates are broadly consistent with those in the literature. Krishnamurthy and Vissing-Jorgensen (2011) estimate a cumulative 187*bp* two-day decline in the 10-year TIPS real yield around the first five announcements, almost exactly the same as our estimate. Gagnon et al. (2011) estimate a cumulative 91*bp* one-day decline in the 10-year Treasury yield on all announcement days; we estimate a comparable 119*bp* one-day TIPS decline (not shown in the table), less than the 188*bp* two-day decline as expected if illiquidity during this period caused some delay in price impact. For the March 18, 2009 announcement on which we focus below, D'Amico and King (2013) estimate a one-day decline in the 10-year Treasury yield by more than 50*bp* using the prices of securities which were eventually purchased, only slightly less than the two-day changes in the interpolated TIPS yield curve which we find.

C.4.2 QE in model

We now describe how we simulate QE in the model.

We focus for concreteness on the March 18, 2009 announcement that the Federal Reserve would begin purchasing up to $300bn of longer-term Treasuries and increase the size of agency/GSE-backed debt and agency MBS purchases up to $200bn and

$1.25tn, respectively.[77] Prior to this announcement, the Federal Reserve had only announced that it "could" purchase Treasuries without specifying that it would, and it had announced (on November 25, 2008) that it would purchase up to $100bn and $500bn in agency/GSE-backed debt and agency MBS, respectively.

In the model simulation we thus assume that all of the purchases of Treasuries from April 2009 through March 2010 were unanticipated prior to the announcement, and that $100bn and $750bn of the purchases of agency/GSE-backed debt and agency MBS over this period were unanticipated.[78] We further assume that, upon announcement, agents assume that the assets will roll off the Federal Reserve's balance sheet simply as they mature. To the extent that some of these purchases were in fact anticipated, or agents expected the assets to be sold off the balance sheet more quickly, it will mean we overestimate $\alpha(\tau)$ in our calibration.

Simulating these asset purchases requires translating them into model scale. We use the following moments. Over the 2012-2019 period overlapping with our maintained sample period of interest, the total assets of broker/dealers and hedge funds as measured using the approach in Table 2 were 30% of annual U.S. GDP.[79] Thus, in the model, we assume that in month 0, agents learn that habitat demand at maturity τ at time t will fall by an amount

$$\frac{\text{purchases}(\tau)_t}{\text{gdp}_{2007}} \frac{\int_0^\infty X^{(\tau)} d\tau}{0.30},$$

where $\text{purchases}(\tau)_t$ is the observed value of asset purchases t months after April 2009 in the data, gdp_{2007} is annual GDP prior to the crisis, and $\int_0^\infty X^{(\tau)} d\tau$ is the average value of arbitrageur assets in the model.

Finally, we must set the initial conditions in the model simulation to associate with March 2009. In particular, we account for the fact that arbitrageurs had lost substantial

[77] To the extent the subsequent announcements in 2009 had small effects because they were partially anticipated, the primary benefit of focusing on this announcement is that it was the "last" unanticipated announcement in the first round of QE. For the earlier announcements, it is more complicated to pin down agents' expected path of purchases following the announcement given that subsequent announcements in fact changed that realized path.

[78] Using our security level purchase data, we estimate $132bn purchases of agency/GSE-backed debt and $967bn purchases of agency MBS over April 2009 through March 2010. We thus multiply each of the purchases of agency/GSE-backed debt and agency MBS purchases over this period by (100/132) and (750/967), respectively, to obtain the unanticipated component of purchases.

[79] Assets refers to all line items in which arbitrageurs are long, e.g. all line items except repo and other short-term loans. Thus, in Q4 2012 for instance, Table 2 demonstrates that arbitrageur assets were $4,291bn.

	Q4 2007	Q1 2009	Percent change
Broker/dealers	285	293	3
Hedge funds	1,975	973	-51
Sum	2,260	1,266	-44

Table 17: change in wealth of arbitrageurs during financial crisis

Notes: all values in nominal $bn. Wealth of broker/dealers defined as described in Table 2. Wealth of hedge funds defined as equity capital reported by He et al. (2010), in turn sourced from Barclay Hedge.

equity capital by this point in the financial crisis. Table 17 summarizes the decline in wealth among broker/dealers and hedge funds from the fourth quarter of 2007 through the first quarter of 2009. While broker/dealer wealth from the Financial Accounts was essentially flat over this period, hedge fund wealth as measured by He et al. (2010) (their Table 4, in turn from Barclay Hedge) fell substantially.[80] We estimate that the total wealth of arbitrageurs fell by 44% over this period. To avoid conveying the impression that this number is very precisely estimated, we thus initialize arbitrageur wealth to one third less than its average value.

We set the other state variables, ω_1 and ω_2, to their average values (zero). These are only important for our simulation of QE insofar as they govern the magnitude of arbitrageurs' carry trades and thus the duration of their wealth. By setting $\omega_1 = \omega_2 = 0$, the model-implied duration of arbitrageurs is roughly double its average value. This in turn implies term premia roughly double their average values, according well with estimates from models maintained by the Federal Reserve or Federal Reserve Bank of New York. We thus set $\omega_1 = \omega_2 = 0$ for simplicity, without further refinement.

The solid line in Figure 6 in the main text summarizes the resulting paths of habitat demand, the yield curve at selected maturities, and arbitrageur wealth in our simulation of QE. The exogenous component of habitat demand eventually falls by more than 40% given the Federal Reserve's purchases. The response of the five- and 10-year real forward rates on impact are $77bp$ and $56bp$, roughly consistent with the observed responses of $74bp$ and $46bp$ to the March 18, 2009 announcement (reported in Table 16) because α and ξ were calibrated to match these moments.

[80] We use this source, rather than the Form PF data used as our primary source for hedge funds in the main text, since the Form PF data is not available prior to 2012.

C.5 Alternative calibrations

In this appendix we report results under a variety of alternative calibrations referenced in the main text. Tables 18-20 describe the calibrated parameters, and Figure 17 depicts for each alternative calibration the response of the forward curve to the same surprise monetary tightening simulated in Figure 4 for the baseline calibration.

Dropping 7/2008-6/2010 yield curve data The baseline model is calibrated to match yield curve moments over our maintained 2004-2019 sample period. Prior work has documented large movements in TIPS liquidity premia around the global financial crisis (e.g., D'Amico et al. (2018)). While our model would imply large conditional movements in TIPS yields during this period arising from low levels of arbitrageur wealth, it is not equipped to speak about liquidity frictions per se. Thus, for robustness purposes, here we consider an alternative calibration to yield curve moments excluding the period July 2008 through June 2010.

Table 18 reports the targets and calibrated parameters in this case. Only the targets in the first panel are different than in the baseline model.[81] As is evident from Figure 17, the effects of a monetary tightening are very similar to those in the baseline calibration.

No arbitrageur balance sheet data We discipline the revaluation of arbitrageurs' wealth upon a monetary shock in our model by matching the evidence assembled in section 4.2 on dealers' and hedge funds' duration. As acknowledged in the main text, none of these estimates are perfect. For this reason, here we present an alternative calibration which avoids using these estimates of duration entirely.

In particular, we exploit the insight that the endogeneity of arbitrageurs' wealth allows our model to generate stochastic volatility in the yield curve, despite homoskedastic driving forces. Thus, rather than calibrating arbitrageurs' initial endowment $\bar{W}$ to match a target for average duration, we calibrate it to match the monthly volatility of daily volatility within each month of the 10-year real yield. Table 19 reports the targets and calibrated parameters in this case.

The key difference from the baseline calibration is that arbitrageurs' duration is in fact higher — around 30 — to match the observed volatility in daily volatility of the

[81] In particular, we continue to calibrate α and ξ to match the high-frequency responses of the forward curve to the QE announcement on March 18, 2009. While these may also reflect the response of liquidity premia, we have already demonstrated the sensitivity of our results to α in the main text.

	Description	Value	Moment	Target	Model
Unconditional moments of yield curve, excluding 7/2008-6/2010					
$\bar{r}$	mean short rate	-0.0035	$y_t^{(5)}$	0.39%	0.42%
γ	arb. risk aversion	4.3	$y_t^{(10)} - y_t^{(5)}$	0.52%	0.52%
κ_1	mean rev. transitory shock	0.10	$\sigma(y_t^{(5)})$	1.05%	1.01%
$\sigma_{r,1}$	short rate transitory loading	0.0087	$\sigma(\Delta y_t^{(5)})$	0.72%	0.72%
$\sigma_{\beta,1}$	demand transitory loading	-0.46	$\beta_{FB}^{(5)}$	0.05	-0.06
κ_2	mean rev. persistent shock	0.03	$\sigma(y_t^{(10)})$	0.86%	0.88%
$\sigma_{r,2}$	short rate persistent loading	0.0050	$\sigma(\Delta y_t^{(10)})$	0.62%	0.63%
$\sigma_{\beta,2}$	demand persistent loading	0.21	$\beta_{FB}^{(10)}$	0.16	0.10
Duration of arbitrageurs					
$\bar{W}$	arb. endowment	0.05	duration	10	9.9
Yield curve responses to QE announcement on March 18, 2009					
α	habitat price elast.	4	$df_t^{(4,5)}$	-0.74%	-0.75%
ξ	persistence arb. wealth	0.1	$df_t^{(9,10)}$	-0.46%	-0.53%

Table 18: alternative calibration: dropping 7/2008-6/2010

Notes: Δ denotes annual change, σ denotes monthly standard deviation, d denotes instantaneous change, and moments without these symbols are simple time-series averages. Model moments are computed as in Table 4.

10-year real yield. In other words, the extent of stochastic volatility in the baseline calibration is too low.[82] As is evident from Figure 17, the effects of a monetary tightening on real forwards are thus substantially amplified versus the baseline calibration. We note that arbitrageur duration of 30 is also consistent with (though at the upper end of) the range we estimate using balance sheet data in section 4.2.

Nonzero $\sigma_{\gamma,1}$ In our baseline calibration, habitat demand loads on the transitory latent state variable with the opposite sign as the short rate. This is required by the data to quantitatively account for the fact that a low short rate is associated with a

[82]Indeed, it is because this calibration features higher arbitrageur duration that the model-implied Fama and Bliss (1987) coefficient for the 10-year bond in Table 19 is lower than in the data. As discussed in footnote 51, the wealth revaluation upon interest rate movements induce negative Fama and Bliss (1987) coefficients. While demand movements can increase these coefficients, the numerical solution becomes unstable when their volatility becomes too large. While we cannot solve the model in a parameter space that matches the observed Fama and Bliss (1987) coefficient for the 10-year bond, we note that the model moment is still within the confidence bounds of the empirical estimate.

	Description	Value	Moment	Target	Model
Unconditional moments of yield curve					
$\bar{r}$	mean short rate	-0.0020	$y_t^{(5)}$	0.51%	0.51%
γ	arb. risk aversion	1.2	$y_t^{(10)} - y_t^{(5)}$	0.52%	0.53%
κ_1	mean rev. transitory shock	0.10	$\sigma(y_t^{(5)})$	1.08%	1.07%
$\sigma_{r,1}$	short rate transitory loading	0.0080	$\sigma(\Delta y_t^{(5)})$	0.85%	0.77%
$\sigma_{\beta,1}$	demand transitory loading	-0.45	$\beta_{FB}^{(5)}$	-0.06	-0.15
κ_2	mean rev. persistent shock	0.03	$\sigma(y_t^{(10)})$	0.89%	0.97%
$\sigma_{r,2}$	short rate persistent loading	0.0050	$\sigma(\Delta y_t^{(10)})$	0.67%	0.70%
$\sigma_{\beta,2}$	demand persistent loading	0.27	$\beta_{FB}^{(10)}$	0.14	-0.30
Stochastic volatility in yield curve					
$\bar{W}$	arb. endowment	-0.10	$\sigma(\sigma_t^d(y_t^{(10)}))$	0.05%	0.04%
Yield curve responses to QE announcement on March 18, 2009					
α	habitat price elast.	4	$df_t^{(4,5)}$	-0.74%	-0.65%
ξ	persistence arb. wealth	0.04	$df_t^{(9,10)}$	-0.46%	-0.43%

Table 19: alternative calibration: no arbitrageur balance sheet data

Notes: Δ denotes annual change, σ denotes monthly standard deviation, d denotes instantaneous change, σ^d denotes daily standard deviation over a month, and moments without these symbols are simple time-series averages. Model moments are computed as in Table 4.

high term premium, as reflected in future excess returns.

However, this is inconsistent with the observed comovements with dealers' balance sheets. In particular, using the Primary Dealer Statistics, we construct the log total position of dealers in Treasuries, TIPS, agency securities, mortgage-backed securities, and corporate bonds, multiplied by 100 and denoted $LOGPOS_t$. We project weekly changes in this measure on weekly changes in the 10-year/two-year real term spread, obtaining a coefficient of -6.3 over our sample period. This means that a $1pp$ higher term spread is associated with $6.3pp$ lower (fixed income) assets on dealers' balance sheets. This is closely related to the finding in Hanson and Stein (2015) that a higher nominal term spread is associated with a lower value of $NETDUR_t$ on dealers' balance sheets (see Table 8 in that paper). Running the same regression on model-generated data instead yields a positive coefficient because $\sigma_{\beta,1} < 0$: habitat demand for borrowing is high when the short rate is low and thus the term spread is high.

There are two natural ways to enrich the model to resolve this shortcoming. One is

	Description	Value	Moment	Target	Model
Unconditional moments of yield curve					
$\bar{r}$	mean short rate	-0.0035	$y_t^{(5)}$	0.51%	0.52%
γ	mean arb. risk aversion	3	$y_t^{(10)} - y_t^{(5)}$	0.52%	0.54%
κ_1	mean rev. transitory shock	0.10	$\sigma(y_t^{(5)})$	1.08%	1.08%
$\sigma_{r,1}$	short rate transitory loading	0.0085	$\sigma(\Delta y_t^{(5)})$	0.85%	0.81%
$\sigma_{\beta,1}$	demand transitory loading	0.07	see text	-6.3	-5.2
$\sigma_{\gamma,1}$	risk aversion transitory loading	-0.80	$\beta_{FB}^{(5)}$	-0.06	-0.17
κ_2	mean rev. persistent shock	0.03	$\sigma(y_t^{(10)})$	0.89%	1.02%
$\sigma_{r,2}$	short rate persistent loading	0.0054	$\sigma(\Delta y_t^{(10)})$	0.67%	0.77%
$\sigma_{\beta,2}$	demand persistent loading	0.19	$\beta_{FB}^{(10)}$	0.14	0.21
Duration of arbitrageurs					
$\bar{W}$	arb. endowment	0.06	duration	10	11.4
Yield curve responses to QE announcement on March 18, 2009					
α	habitat price elast.	4	$df_t^{(4,5)}$	-0.74%	-0.40%
ξ	persistence arb. wealth	0.1	$df_t^{(9,10)}$	-0.46%	-0.23%

Table 20: alternative calibration: nonzero $\sigma_{\gamma,1}$

Notes: Δ denotes annual change, σ denotes monthly standard deviation, d denotes instantaneous change, and moments without these symbols are simple time-series averages. Model moments are computed as in Table 4.

to consider "news" shocks to the short rate, as would be implied in general equilibrium by news about future growth. News about higher future short rates (leaving the current short rate unchanged) imply a steeper yield curve, lower arbitrageur assets, and higher future excess returns on long-term bonds. The wealth revaluation mechanism is essential here, as it implies that arbitrageurs incur balance sheet losses on long-term bonds arising from such news shocks. Another is to consider shocks to arbitrageurs' effective risk aversion, as by losses on other parts of their portfolio that affect their wealth. Intuitively, if arbitrageurs get more risk averse, it causes the term spread to widen, their balance sheets to shrink, and future excess returns to be high.

We present a calibration along the second dimension here to assess its quantitative properties. For expositional simplicity we model shocks to risk aversion γ_t directly, though it would be straightforward to instead add an additional shock to arbitrageurs' wealth. We discipline the loading of habitat demand on the transitory factor $\sigma_{\beta,1}$ to

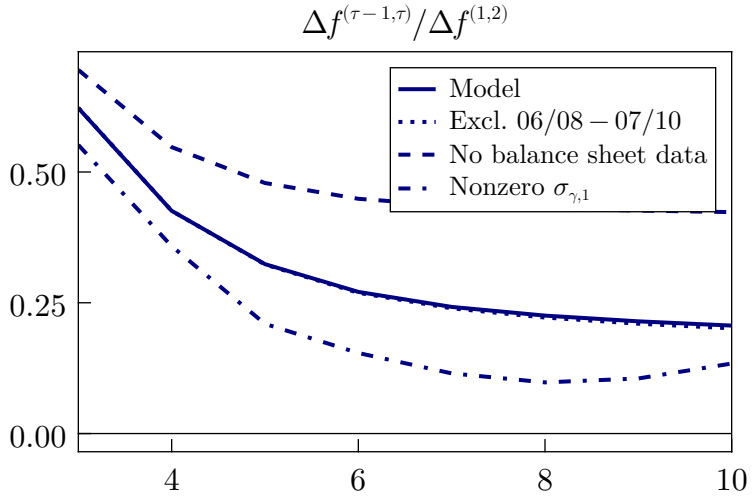

Figure 17: $f_t^{(\tau-1,\tau)}$ on $f_t^{(1,2)}$ given monetary shock: alternative calibrations

Notes: responses simulated as described in Figure 2.

match the comovement of arbitrageurs' assets with the term spread, and the loading of log risk aversion on the transitory factor $\sigma_{\gamma,1}$ to match the five-year Fama and Bliss (1987) coefficient.[83] We assume that risk aversion only loads on the transitory factor, so $\sigma_{\gamma,2} = 0$. Table 20 reports the targets and calibrated parameters in this case. We note that this calibration thus accounts for the evidence in Hanson and Stein (2015) without requiring "reach for yield" behavior on the part of habitat investors.

Figure 17 demonstrates that a monetary tightening implies a smaller increase in term premia in this case than in the baseline model. This is because the overreaction to monetary shocks is especially high in high-duration states, and duration does not vary by as much. This in turn is because risk premium fluctuations are now generated more by movements in risk aversion, and less by movements in demand. Nonetheless, we underscore that this environment still features "overreaction" of forward rates to monetary shocks arising from the wealth revaluation channel.

C.6 Consumption through life and finite ρ

The environment studied in the paper makes two assumptions — that arbitrageurs only consume upon death, and that their discount factor $\rho \to \infty$ — that allow us

[83] As noted in footnote 46, the five-year Fama and Bliss (1987) coefficient is negative only because of Stambaugh (1999) bias. In longer samples, it is positive.

to nest the model of Vayanos and Vila (2021) when arbitrageurs' death probability $\xi \to \infty$. We view this as a valuable feature of our baseline model.

Here we demonstrate that our qualitative and quantitative insights with endogenous wealth (finite ξ) do not rely on these assumptions. We first outline the alternative environment, then characterize the equilibrium and how our numerical algorithm can be modified to solve for it, and finally describe the equilibrium given the same parameters as in our baseline model.

Environment Arbitrageurs consume while they are alive. To avoid discontinuities upon death, we also now assume that arbitrageurs trade in annuities with competitive insurance companies, à la Blanchard (1985). Since arbitrageurs have no bequest motive, they will optimally trade in contracts such that they receive a flow ξdt times their wealth if they remain alive in an interval dt, and leave all of their wealth to the insurance company if they die. Finally, to simplify the solution of the consumption-savings problem while retaining risk aversion as a free parameter, we adopt recursive preferences with a unitary elasticity of intertemporal substitution.[84]

The arbitrageur thus chooses its sequence of consumption and financial portfolios to maximize

$$v_t = \max_{\{c_{t+s}, \{x_{t+s}^{(\tau)}\}\}} E_t \int_0^\infty f\left(c_{t+s}, v_{t+s}\right) ds, \tag{51}$$

where

$$f\left(c, v\right) = (\xi + \rho)(1-\gamma)v \left[\log\left(c\right) - \frac{1}{1-\gamma}\log\left((1-\gamma)v\right)\right], \tag{52}$$

subject to the budget constraint

$$dw_t = w_t(\xi + r_t)dt - c_t dt + \int_0^\infty x_t^{(\tau)} \left(\frac{dP_t^{(\tau)}}{P_t^{(\tau)}} - r_t dt\right) d\tau, \tag{53}$$

which already accounts for the arbitrageur's use of the competitive annuity market to insure against death. This formulation of recursive preferences follows Garleanu and Panageas (2023), with coefficient

[84] Another approach to obtaining a linear consumption-savings policy and portfolio choice similar to the baseline model is to employ log preferences together with a value-at-risk constraint, as demonstrated in Oskolkov (2024). That approach eliminates intertemporal hedging terms from portfolio choice for all values of parameters.

of relative risk aversion γ. Aggregate arbitrageur wealth then follows

$$dW_t = W_t r_t dt - C_t dt + \int_0^\infty X_t^{(\tau)} \left(\frac{dP_t^{(\tau)}}{P_t^{(\tau)}} - r_t dt \right) d\tau + \xi \bar{W} dt. \tag{54}$$

The rest of the environment is as in section 2.

Equilibrium We can characterize the equilibrium using similar steps as in appendix C.1. Given a conjectured value function satisfying

$$v_t = \frac{(\nu_t w_t)^{1-\gamma}}{1-\gamma}, \tag{55}$$

where ν_t does not depend on the arbitrageur's individual level of wealth, it is straightforward to demonstrate that optimal consumption solves

$$c_t = (\xi + \rho) w_t \tag{56}$$

and optimal portfolio choice solves (35) for each $\tau \in (0, \infty)$ as in the baseline model. Aggregation then implies

$$\chi_t^{(\tau)} = \frac{X_t^{(\tau)}}{W_t}, \quad \frac{c_t}{w_t} = \frac{C_t}{W_t}.$$

It follows that the aggregate policies are

$$C_t = (\xi + \rho) W_t \tag{57}$$

and (20) for each $\tau \in (0, \infty)$, respectively. Finally, ν_t solves the PDE

$$\begin{aligned} 0 = & -\kappa_1 \omega_{1,t} \frac{\nu_{1,t}}{\nu_t} - \kappa_2 \omega_{2,t} \frac{\nu_{2,t}}{\nu_t} + \mu_{W,t} \frac{\nu_{W,t}}{\nu_t} \\ & + \frac{1}{2} \left(-\gamma \left(\frac{\nu_{1,t}}{\nu_t} \right)^2 + \frac{\nu_{11,t}}{\nu_t} \right) + \frac{1}{2} \left(-\gamma \left(\frac{\nu_{2,t}}{\nu_t} \right)^2 + \frac{\nu_{22,t}}{\nu_t} \right) \\ & + \frac{1}{2} \left(\eta_{1,t}^2 + \eta_{2,t}^2 \right) \left(-\gamma \left(\frac{\nu_{W,t}}{\nu_t} \right)^2 + \frac{\nu_{WW,t}}{\nu_t} \right) \\ & + \eta_{1,t} \left(-\gamma \frac{\nu_{W,t}}{\nu_t} \frac{\nu_{1,t}}{\nu_t} + \frac{\nu_{W1,t}}{\nu_t} \right) + \eta_{2,t} \left(-\gamma \frac{\nu_{W,t}}{\nu_t} \frac{\nu_{2,t}}{\nu_t} + \frac{\nu_{W2,t}}{\nu_t} \right) \\ & + \left[r_t - \rho + \int_0^\infty \chi_t^{(\tau)} \left(\mu_t^{(\tau)} - r_t \right) d\tau \right] \end{aligned}$$

$$
\begin{aligned}
&- \frac{1}{2}\gamma \left(\left[\int_0^\infty \chi_t^{(\tau)} \eta_{1,t}^{(\tau)} d\tau \right]^2 + \left[\int_0^\infty \chi_t^{(\tau)} \eta_{2,t}^{(\tau)} d\tau \right]^2 \right) \\
&\quad + (1-\gamma) \left[\int_0^\infty \chi_t^{(\tau)} \eta_{1,t}^{(\tau)} d\tau \right] \left[\frac{\nu_{1,t}}{\nu_t} + \eta_{1,t} \frac{\nu_{W,t}}{\nu_t} \right] \\
&\quad + (1-\gamma) \left[\int_0^\infty \chi_t^{(\tau)} \eta_{2,t}^{(\tau)} d\tau \right] \left[\frac{\nu_{2,t}}{\nu_t} + \eta_{2,t} \frac{\nu_{W,t}}{\nu_t} \right] \\
&\qquad + (\xi+\rho)\log(\xi+\rho) - (\xi+\rho)\log\nu_t. \quad (58)
\end{aligned}
$$

Numerical algorithm We follow similar steps as in appendix C.2. The optimal portfolio choice condition (20) can be written as in (38), except the drifts are now

$$
\mu_{1,t}^Q = -\kappa_1 \omega_{1,t} - \frac{\gamma}{W_t}\eta_{1,t} + (1-\gamma)\left(\frac{\nu_{1,t}}{\nu_t} + \eta_{1,t}\frac{\nu_{W,t}}{\nu_t} \right), \quad (59)
$$

$$
\mu_{2,t}^Q = -\kappa_2 \omega_{2,t} - \frac{\gamma}{W_t}\eta_{2,t} + (1-\gamma)\left(\frac{\nu_{2,t}}{\nu_t} + \eta_{2,t}\frac{\nu_{W,t}}{\nu_t} \right), \quad (60)
$$

$$
\begin{aligned}
\mu_{W,t}^Q = \mu_{W,t} &- \frac{\gamma}{W_t}\left(\eta_{1,t}^2 + \eta_{2,t}^2 \right) \\
&+ (1-\gamma)\eta_{1,t}\left(\frac{\nu_{1,t}}{\nu_t} + \eta_{1,t}\frac{\nu_{W,t}}{\nu_t} \right) + (1-\gamma)\eta_{2,t}\left(\frac{\nu_{2,t}}{\nu_t} + \eta_{2,t}\frac{\nu_{W,t}}{\nu_t} \right), \quad (61)
\end{aligned}
$$

given unchanged expressions for $\eta_{1,t}$ and $\eta_{2,t}$ in (47) and (48), and

$$
\begin{aligned}
\mu_{W,t} = &\ \xi\left(\bar{W} - W_t \right) - \rho W_t \\
&+ W_t r_t + \int_0^\infty \left(\alpha(\tau)\log\left(P_t^{(\tau)} \right) + \theta_0(\tau) + \theta_1(\tau)\beta_t \right)\left(\mu_t^{(\tau)} - r_t \right) d\tau. \quad (62)
\end{aligned}
$$

Using the Feynman-Kac formula, the solution is as in (42).

The difficulty relative to the baseline model is that we need to solve for ν_t together with the equilibrium price function. Rather than focusing on the PDE (58), we find it much faster to focus on equations (51) and (52) in equilibrium. Given aggregation, we can express (52) in terms of aggregate consumption and wealth. Using the form of the value function (55) and equilibrium consumption in (57), we have

$$
\begin{aligned}
f(C_t, V_t) &= (\xi+\rho)(1-\gamma)V_t \left[\log(C_t) - \frac{1}{1-\gamma}\log\left((1-\gamma)V_t \right) \right] \\
&= (\xi+\rho)\left(\nu_t W_t \right)^{1-\gamma} \left[\log(\xi+\rho) + \log W_t - \frac{1}{1-\gamma}\log\left(\left(\nu_t W_t \right)^{1-\gamma} \right) \right] \\
&= (\xi+\rho)\left(\nu_t W_t \right)^{1-\gamma} \left[\log(\xi+\rho) - \log\nu_t \right]. \quad (63)
\end{aligned}
$$

Combining with (51) and (55), we then obtain

$$(\nu_t W_t)^{1-\gamma} = (\xi+\rho)(1-\gamma)E_t \int_0^\infty (\nu_{t+s} W_{t+s})^{1-\gamma} \left[\log(\xi+\rho) - \log \nu_{t+s}\right] ds. \tag{64}$$

This motivates the following computational algorithm, extending that for the baseline model:

1. Create a tensor grid of ω_t, ω_2, and W values.

2. Initialize $\mu_1^Q(\omega_1,\omega_2,W)$, $\mu_2^Q(\omega_1,\omega_2,W)$, $\mu_W^Q(\omega_1,\omega_2,W)$, $\mu_W(\omega_1,\omega_2,W)$, $\eta_1(\omega_1,\omega_2,W)$, $\eta_2(\omega_1,\omega_2,W)$, and $\nu(\omega_1,\omega_2,W)$ at each grid point. In the first iteration, set them to zero except for $\nu(\omega_1,\omega_2,W)$ which we set to 1.

3. Use cubic splines to approximate $\mu_1^Q(\omega_1,\omega_2,W)$, $\mu_2^Q(\omega_1,\omega_2,W)$, $\mu_W^Q(\omega_1,\omega_2,W)$, $\mu_W(\omega_1,\omega_2,W)$, $\eta_1(\omega_1,\omega_2,W)$, $\eta_2(\omega_1,\omega_2,W)$, and $\nu(\omega_1,\omega_2,W)$ outside of the grid points.

4. Approximate (42) using Monte Carlo simulation:

   (a) For each grid point simulate N sequences of ω_1, ω_2, and W of length $\bar{\tau}/dt$, where dt is the size of the time steps in the simulation. The stochastic processes are approximated using the Euler-Maruyama method.

   (b) Calculate an approximation of the price of a bond of maturity τ at each grid point as

   $$P^{(\tau)}(\omega_1,\omega_2,W) = E_t^Q\left[e^{-\int_0^\tau r_{t+s}ds}|(\omega_1,\omega_2,W)\right] \approx \frac{1}{N}\sum_{n=1}^{N} e^{-\sum_{i=1}^{\tau/dt} r_{n,i}(\omega_1,\omega_2,W)dt},$$

   where $r_{n,i}(\omega_1,\omega_2,W)$ denotes the ith observation in the nth simulation of the interest rate process starting from state (ω_1,ω_2,W) at t (using (6)).

   (c) Given the solution in (c), use equation (64) to calculate an approximation of $\nu(\omega_1,\omega_2,W)$ as

   $$\nu(\omega_1,\omega_2,W) \approx \frac{1}{W}\Bigg[(\xi+\rho)(1-\gamma)\frac{1}{N}\sum_{n=1}^{N}\sum_{i=1}^{\infty}\left(\nu_{n,i}(\omega_1,\omega_2,W)W_{n,i}(\omega_1,\omega_2,W)\right)^{1-\gamma} \times \left[\log(\xi+\rho) - \log \nu_{n,i}(r,\beta,W)\right] dt\Bigg]^{\frac{1}{1-\gamma}},$$

where wealth W_t evolves under the physical measure, i.e.

$$dW_t = \mu_W(\omega_{1,t}, \omega_{2,t}, W_t)dt + \eta_1(\omega_{1,t}, \omega_{2,t}, W_t)dB_{1,t} + \eta_2(\omega_{1,t}, \omega_{2,t}, W_t)dB_{2,t}.$$

5. Update the values for $\mu_1^Q(\omega_1, \omega_2, W)$, $\mu_2^Q(\omega_1, \omega_2, W)$, $\mu_W^Q(\omega_1, \omega_2, W)$, $\mu_W(\omega_1, \omega_2, W)$, $\eta_1(\omega_1, \omega_2, W)$, $\eta_2(\omega_1, \omega_2, W)$, and $\nu(\omega_1, \omega_2, W)$ using (59)-(61), (62), (47)-(48), and the approximation in the previous step.

6. If the values in step 5 are sufficiently close to those guessed in step 2, stop. Otherwise, return to step 2 using the values in step 5.

Calibration and results We use the exact same parameterization as our baseline model in Table 4, except that we set $\rho = 0.01$.[85] Table 21 demonstrates that the equilibrium yield curve is very similar to that in the baseline model. Figure 18 then simulates the same unexpected monetary shock simulated in Figure 3. It demonstrates that the overreaction of forward rates to a monetary shock is comparable to that in the baseline model.

[85]With consumption throughout life, we no longer need arbitrageur death ($\xi > 0$) to keep arbitrageurs' wealth stationary: a sufficiently high discount rate and thus consumption rate could do the same, even with $\xi = 0$. However, we do not explore such a parameterization here.

	Consumption through life and $\rho = 0.01$	Baseline model
$y_t^{(5)}$	0.51%	0.51%
$y_t^{(10)} - y_t^{(5)}$	0.52%	0.52%
$\sigma(y_t^{(5)})$	1.07%	1.06%
$\sigma(y_t^{(10)})$	0.94%	0.94%
$\sigma(\Delta y_t^{(5)})$	0.77%	0.76%
$\sigma(\Delta y_t^{(10)})$	0.67%	0.67%

Table 21: first and second moments of yield curve

Notes: Δ denotes annual change, σ denotes monthly standard deviation, and moments without these symbols are simple time-series averages. Moments are computed as in Table 4.

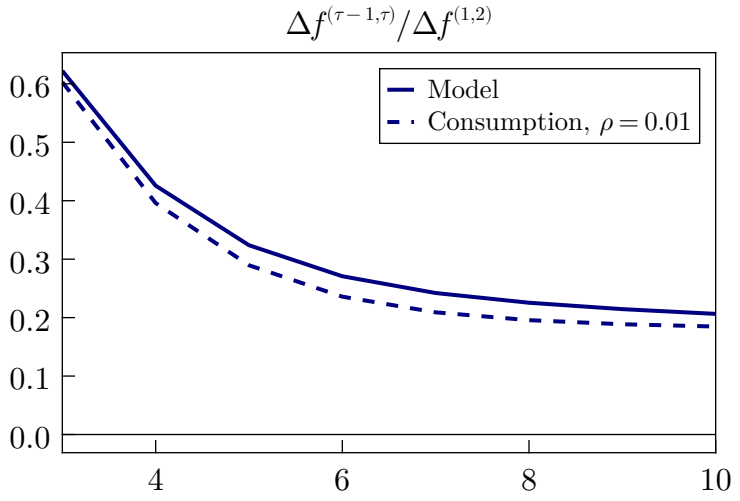

Figure 18: $f_t^{(\tau-1,\tau)}$ on $f_t^{(1,2)}$ given monetary shock

Notes: responses simulated as described in Figure 2.